Gifts of Cosmic Wakefields:

Gamma-ray bursts and cosmic-rays from blazars

Toshiki Tajima

Norman Rostoker Professor, UC Irvine

Riken Seminar
Wako, Japan
Nov. 13, 2018

T. Ebisuzaki, A. Mizuta, S. Horiuchi, K. Abazajian, N. Canac, G. Mourou, K. Nakajima, B. Barish**, R. Matsumoto, K. Shibata, S. Ichimaru, M. Teshima, A. Caldwell, S. Barwick, D. Gilden*

* Nobel Laureate (2018), ** Nobel Laureate (2017)

abstract

1. **Wakefield: robustly elevated** energy state, **relativistic coherence, Higgs' state of plasma ←→Field Reversed Configuration:** robustly elevated energy state

   → **Landau-Ginzburg-like potential**

2. **Wakefield** driven by large clump accreting from the disk toward BH / jets --→ **gamma emissions** that reflect the accretion episode (Ebisuzaki; Mizuta; Abazajian)

3. Accreting clump to induce **gradvitational wave emission (GWE)**

4. More intense case: jet formation by **colliding 2 NS** (Takahashi-Tajima, 2000) or BH's → jet formation

5. Fermi acceleration → **Wakefield acceleration**

Elements of Wakefields

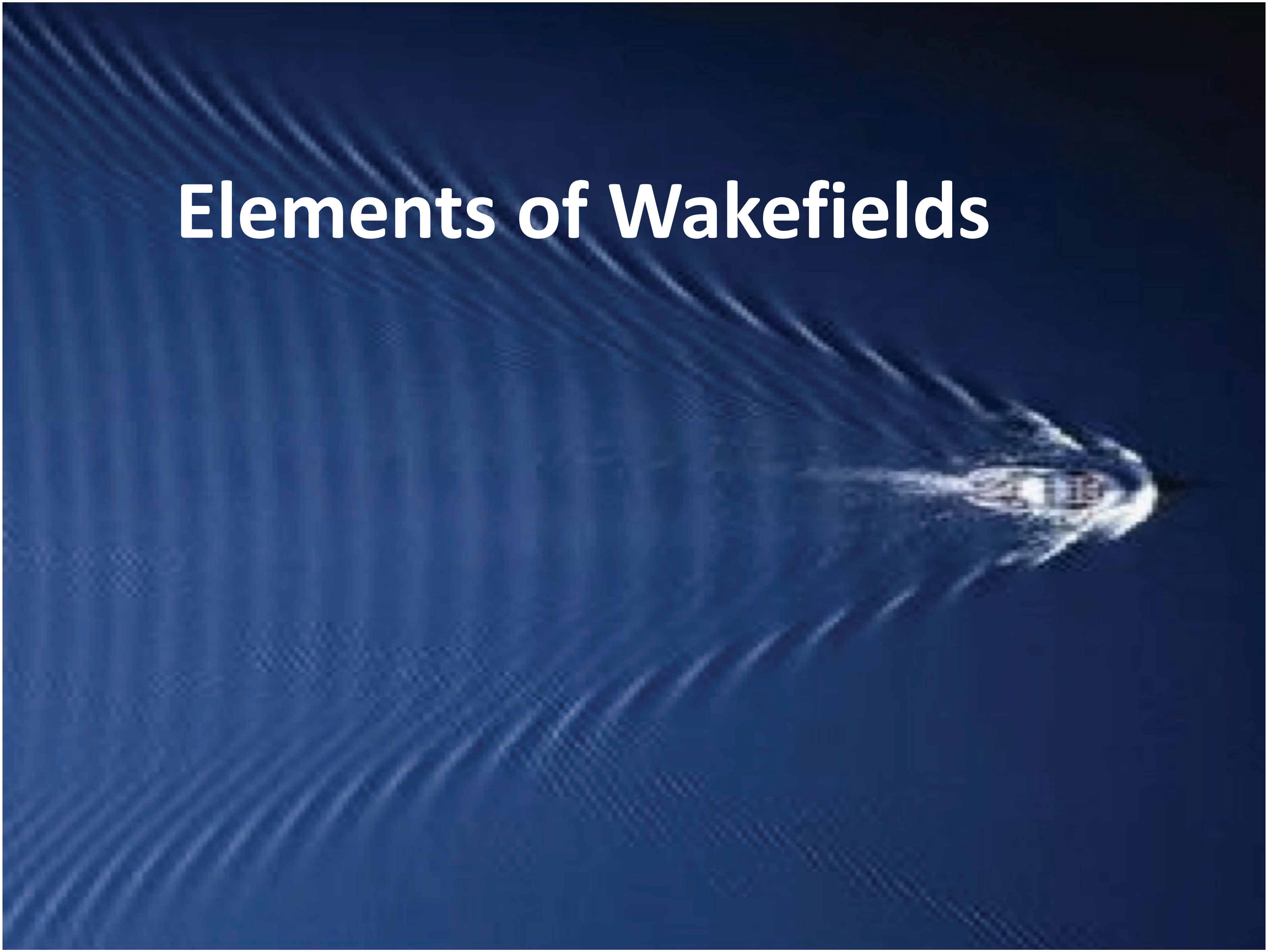

Laser Wakefield (LWFA):

Wake phase velocity >> water movement speed
maintains **coherent** and **smooth** structure

Tsunami phase velocity becomes ~0,
causes **wavebreak** and **turbulence**

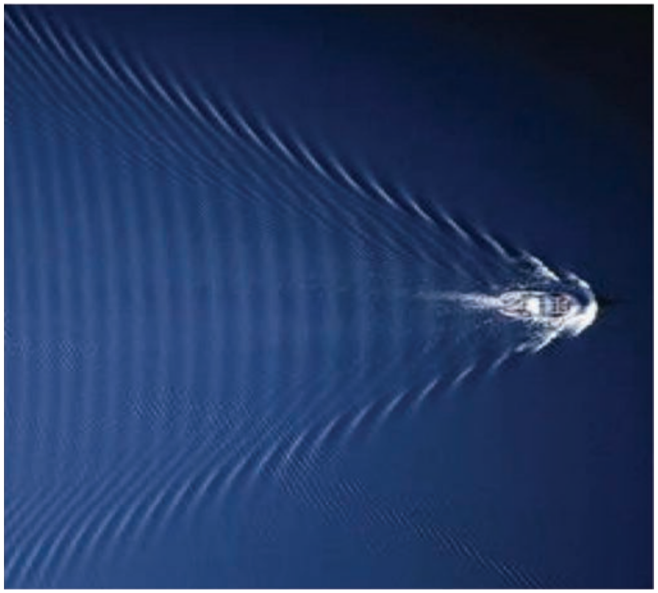

vs

Strong beam (of laser / particles) drives plasma waves to saturation amplitude: $E = m\omega v_{ph} / e$

No wave breaks and wake **peaks** at v≈c

Wave **breaks** at v<c

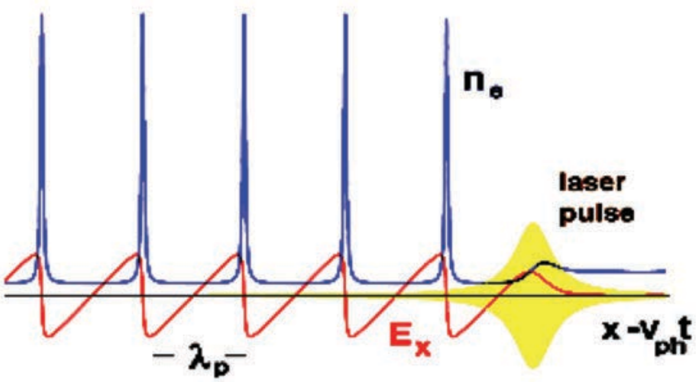

← relativity regularizes (*relativistic coherence*)

Relativistic coherence enhances beyond the Tajima-Dawson field $E = m\omega_p c / e$ (~ GeV/cm)

<u>Relativistic</u> nonlinearity under intense waves

Plasma free of binding potential , but its electron responses forms its sturdy “spine”:

a) Classical EM : $v_{os} << c$,

$a_0 << 1$: δx only

b) <u>Relativistic</u> EM: $v_{os} \sim c$

$a_0 >> 1$: $\delta z >> \delta x$

$$a_0 = \frac{eA_0}{mc^2} = \frac{eE_0\lambda}{mc^2}$$

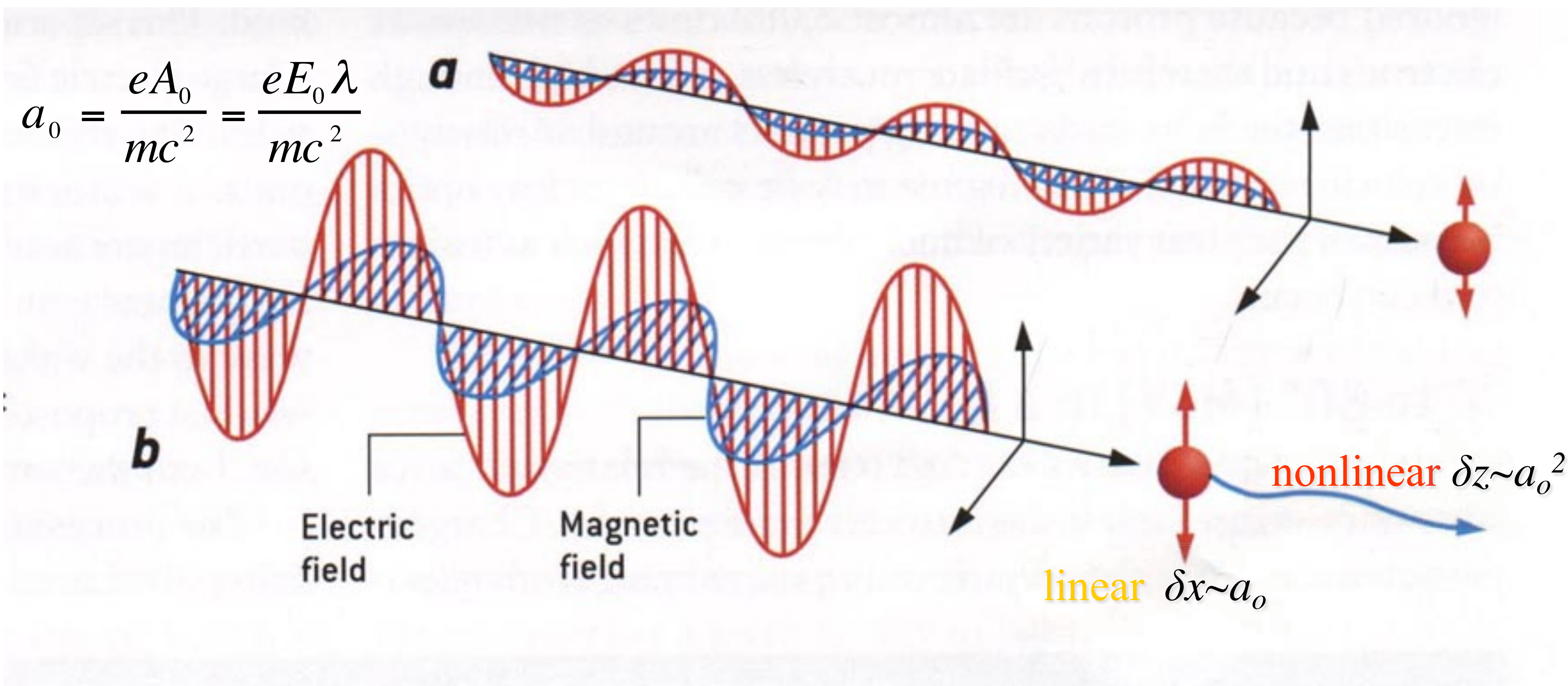

Thermal plasma vs. Wakefields (and Higgs)

Trivial vacuum vs. Laundau-Ginzburg potential → BCS → Nambu → Higgs vacuum
Thermal plasma and Landau damping → wakefields , plasma with elevated energy
Thermal plasma → Field Reversed Configuration plasma

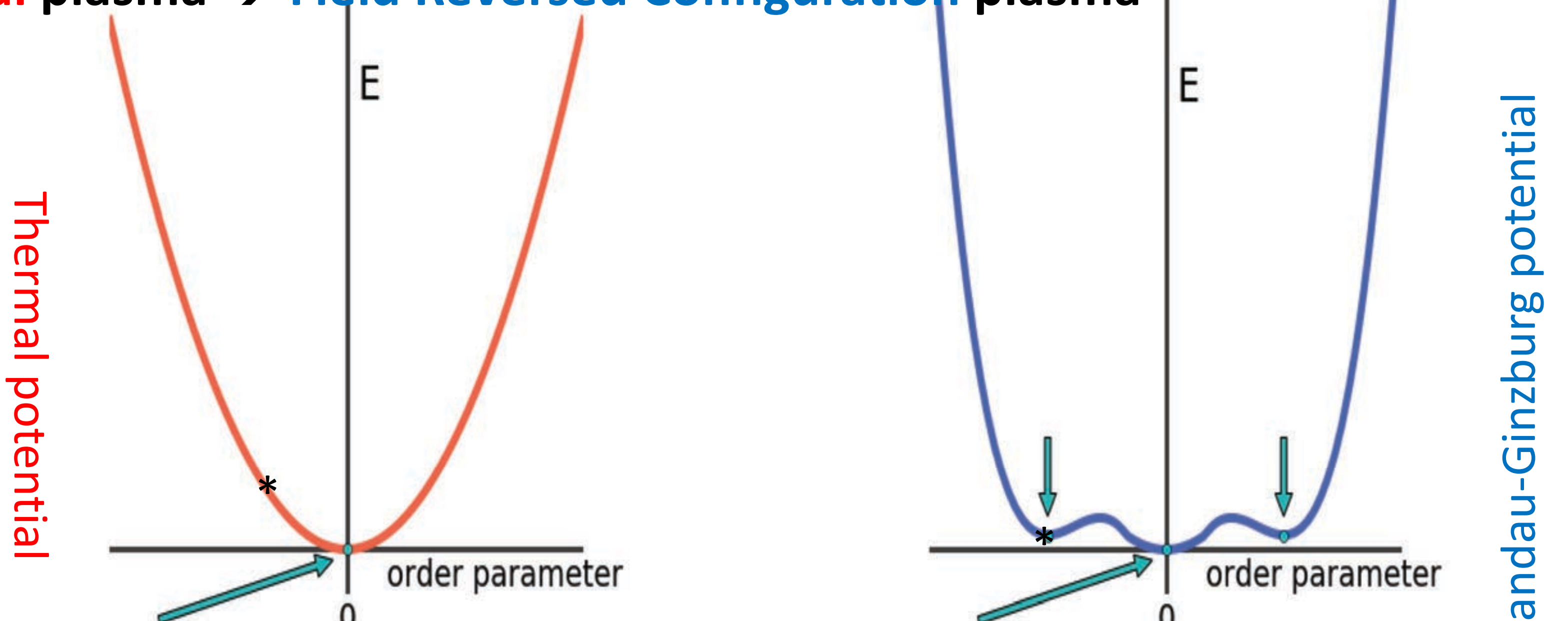

[**Landau damping**: decay of excited waves to equilibrium (left picture)]

Wakefield: no damping; distinct excited <u>stable state</u> ←no particles to resonate (@ $v_{ph} >> v_{th}$)
= plasma's elevated Higgs state , "onigokko (hide 'n seek)" state , or "spined" state

| 0 > vs. | *H* > (cf . | *H* > → | 0 >)

thermo-equilibrium — wakefield state — tsunami onshore

Tajima, Nakajima, Mourou*, RNC (2017)

GeV electrons from a centimeter LWFA

(a slide given to me by S. Karsch)

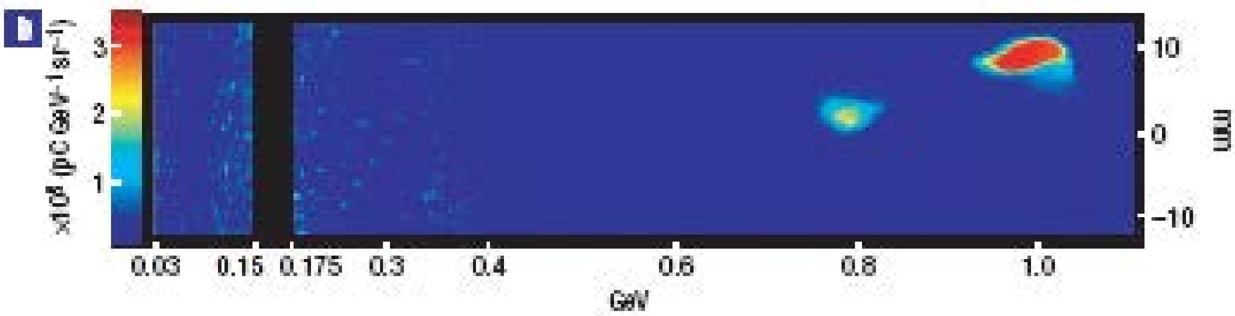

Leemans et al., Nature Physics, september 2006

310-μm-diameter channel capillary

P = 40 TW

density 4.3×10^{18} cm^{-3}.

laser intensity 10^{18} W/cm^2

VOLUME 43, NUMBER 4 PHYSICAL REVIEW LETTERS 23 JULY 1979

Laser Electron Accelerator

T. Tajima and J. M. Dawson

Department of Physics, University of California, Los Angeles, California 90024

(Received 9 March 1979)

An intense electromagnetic pulse can create a weak of plasma oscillations through the action of the nonlinear ponderomotive force. Electrons trapped in the wake can be accelerated to high energy. Existing glass lasers of power density 10^{18}W/cm^2 shone on plasmas of densities 10^{18} cm^{-3} can yield gigaelectronvolts of electron energy per centimeter of acceleration distance. This acceleration mechanism is demonstrated through computer simulation. Applications to accelerators and pulsers are examined.

(emphasis by S. Karsch)

Theory of wakefield toward extreme energies

$$\Delta E \approx 2m_0c^2a_0^2\gamma_{ph}^2 = 2m_0c^2a_0^2\left(\frac{n_{cr}}{n_e}\right),$$ (when 1D theory applies)

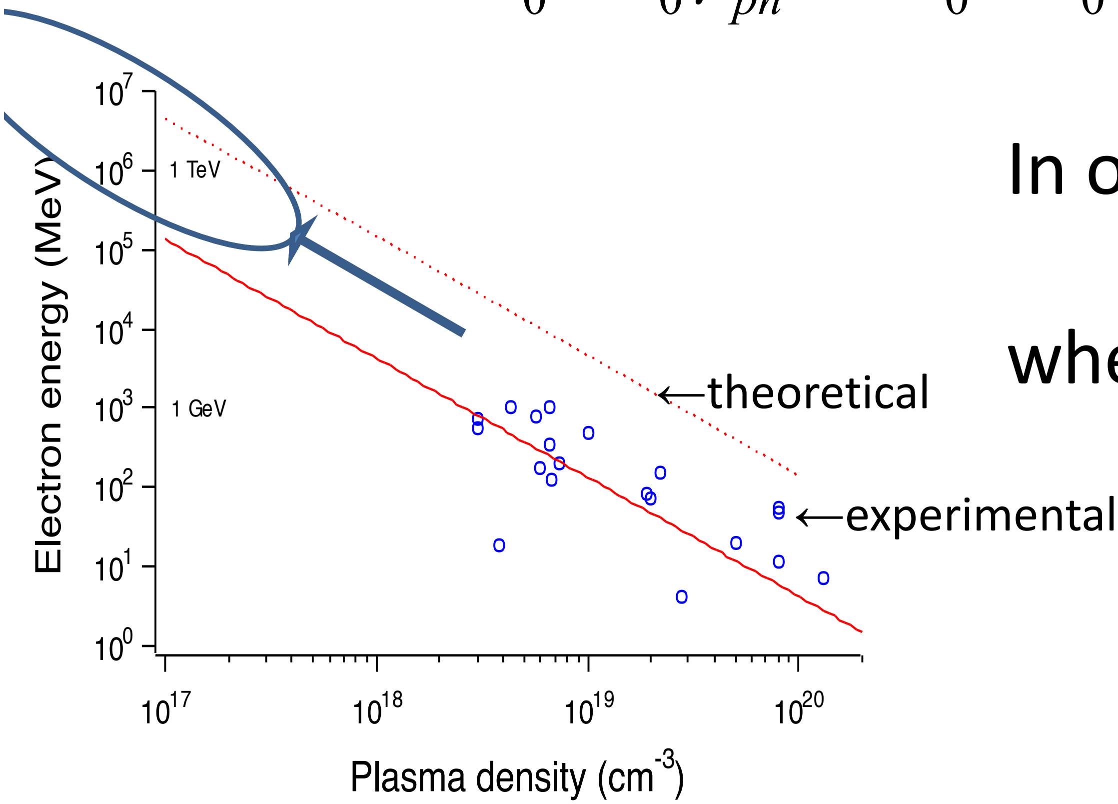

In order to avoid wavebreak,

$$a_0 < \gamma_{ph}^{1/2},$$

where

$$\gamma_{ph} = (n_{cr} / n_e)^{1/2}$$

$n_{cr} = 10^{21}$

$n_e = 10^{16}$

$$L_d = \frac{2}{\pi}\lambda_p a_0^2\left(\frac{n_{cr}}{n_e}\right),$$

dephasing length

$$L_p = \frac{1}{3\pi}\lambda_p a_0\left(\frac{n_{cr}}{n_e}\right),$$

pump depletion length

Superintense Alfven Shock in the Blackhole Accretion Disk
Bow/Wakefield Acceleration toward ZeV Cosmic Rays

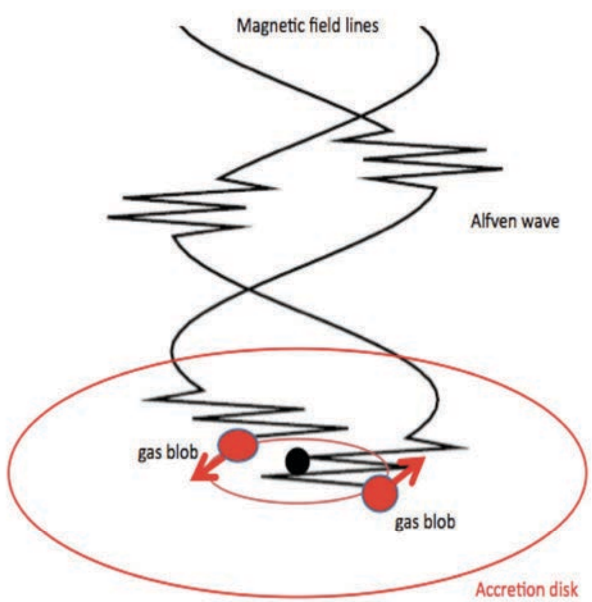

3D bow structure

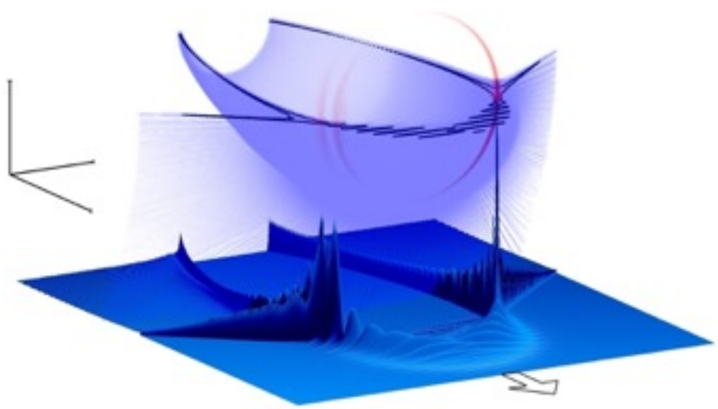

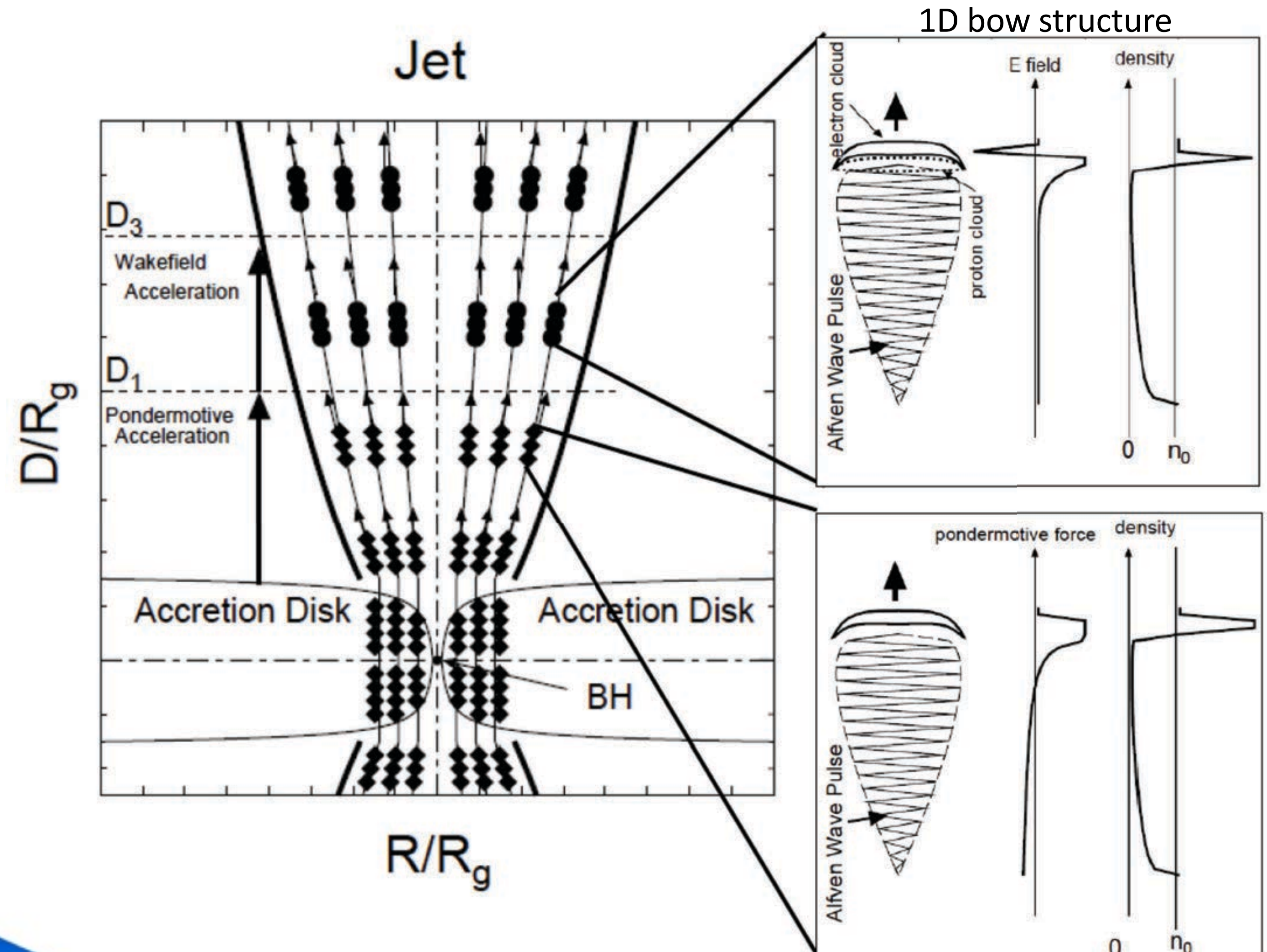

Ebisuzaki and Tajima (2014)

Bow **wake** acceleration

linear acceleration by electrostatic field

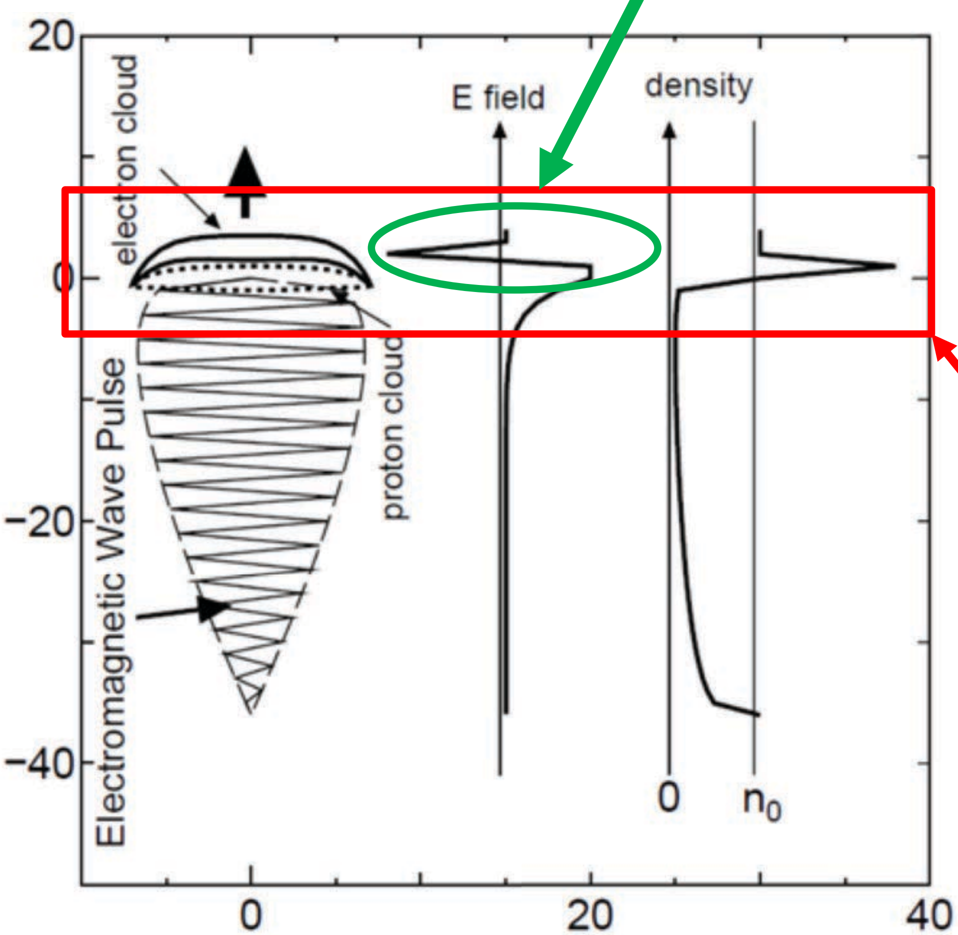

Bow wake

One of the wakefield acceleration, which takes place when a_0>>1

Q: Why do geese fly in the V-shape?

A: Geese fly in the “wake”of the lead goose to ride on the wave (= wakefield acceleration).

Nature's Natural Wakefields: jet wakfields driven by disk MRI instability

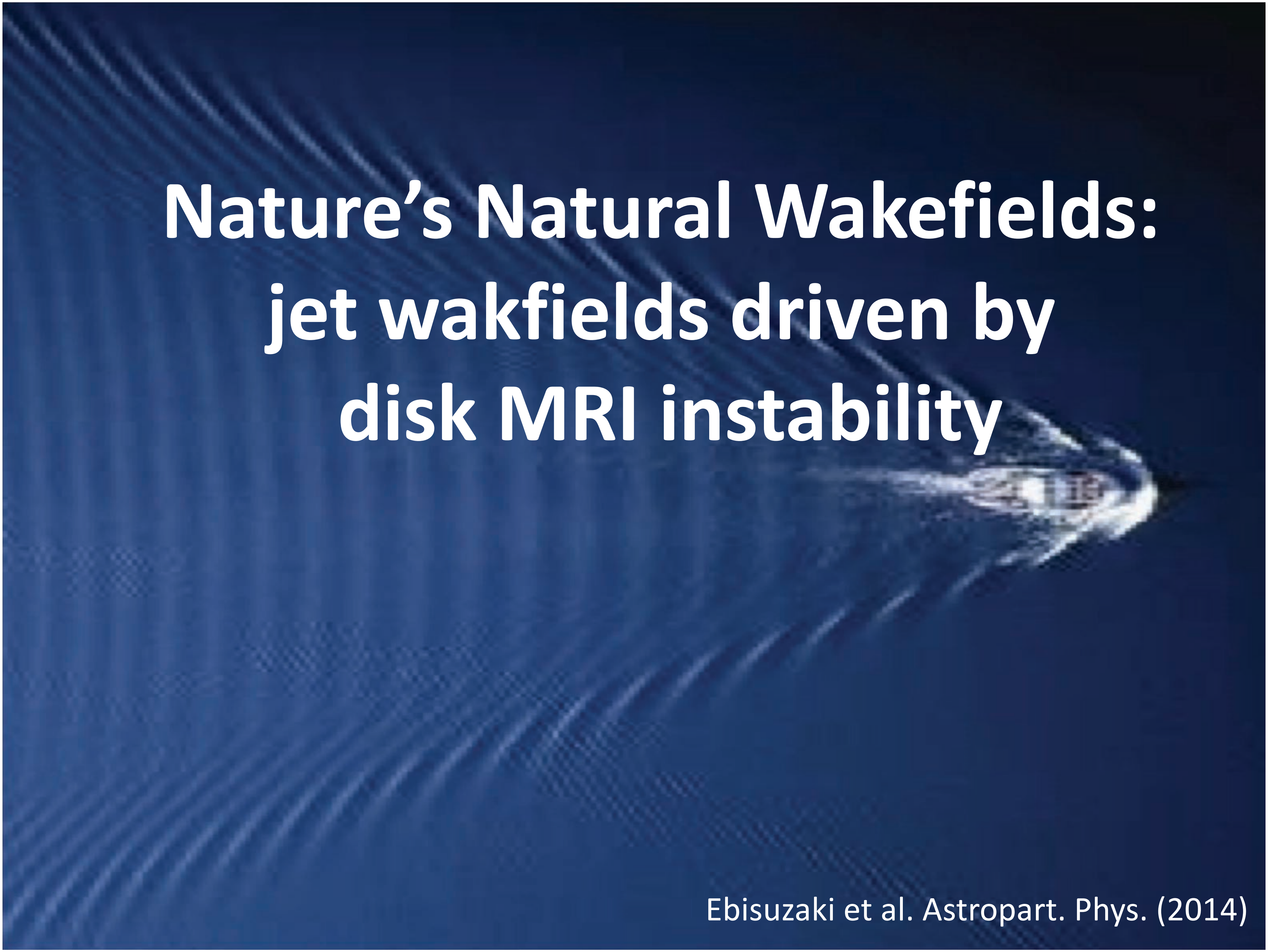

Ebisuzaki et al. Astropart. Phys. (2014)

Enhanced energy emission of jets and wakefields by merging two NS's (or BH's) (Takahashi, Hillman, Tajima, 2000)

in High Field Science, Eds., T. Tajima, K., Mima, and H. Baldis (Kluwer, NY, 2000).p177.

Relativistic Lasers and High Energy Astrophysics 183

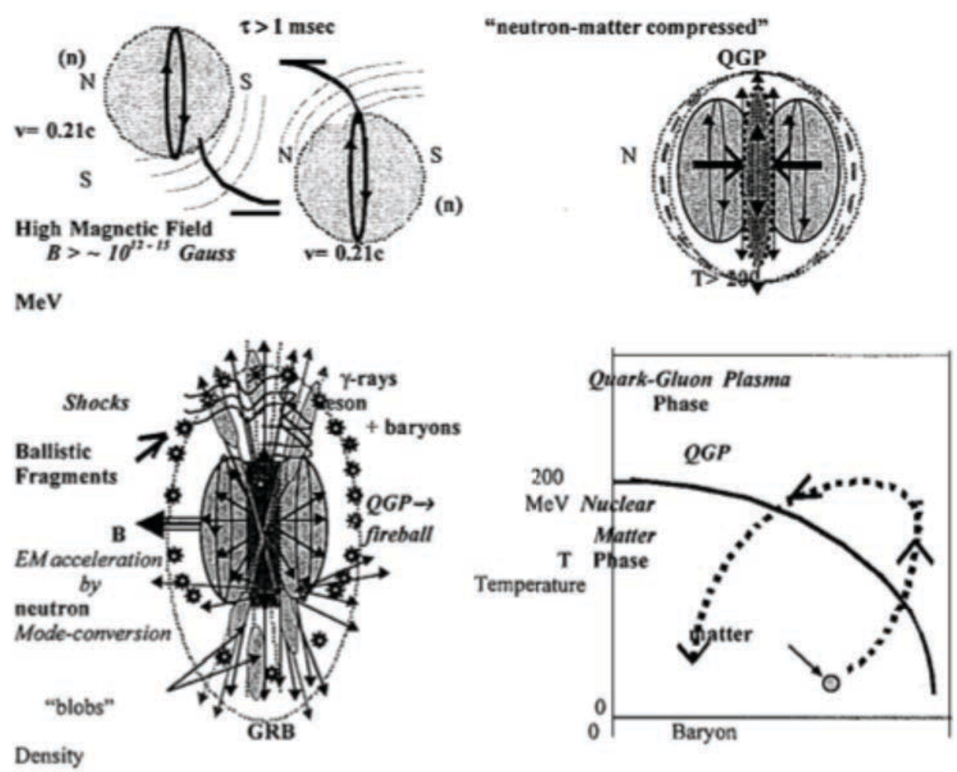

Figure 2. Schematic illustrations of QGP formation in the merge of spinning neutron stars.

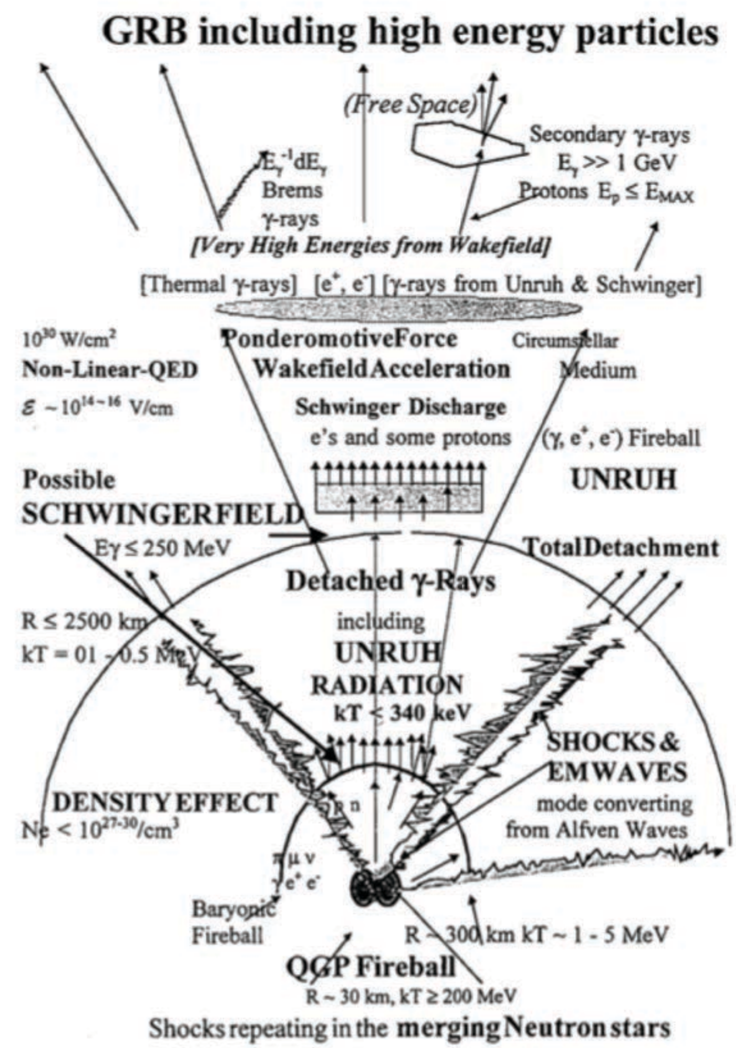

Figure 8. A schematic illustration of the proposed concept.

→ Chen, Tajima, and Takahashi, PRL (2002); Ebisuzaki-Tajima Ap. P (2014)

Eruption of magnetic field in an accretion disk

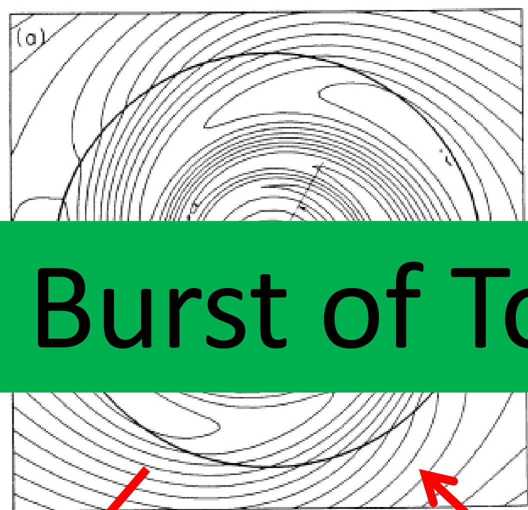

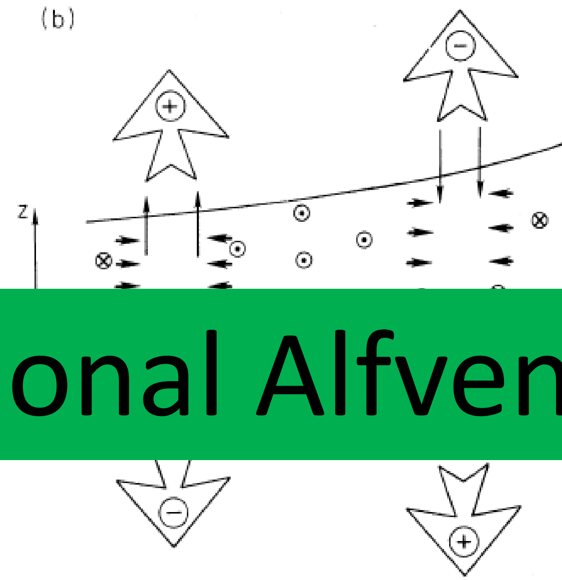

A Burst of Torsional Alfven Waves

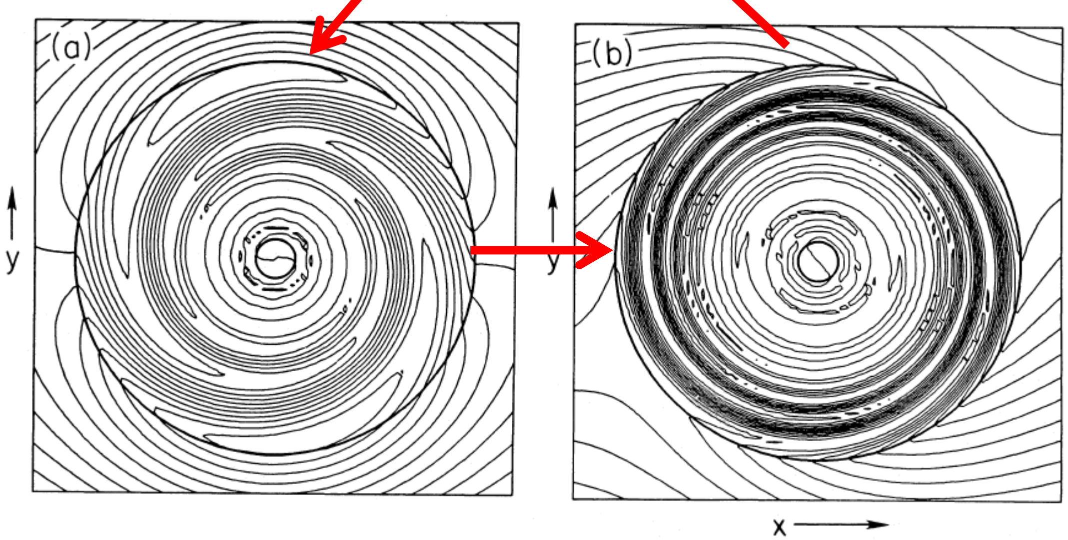

Tajima and Gilden 1987, ApJ
Haswell, Tajima, and Sakai, 1992, ApJ

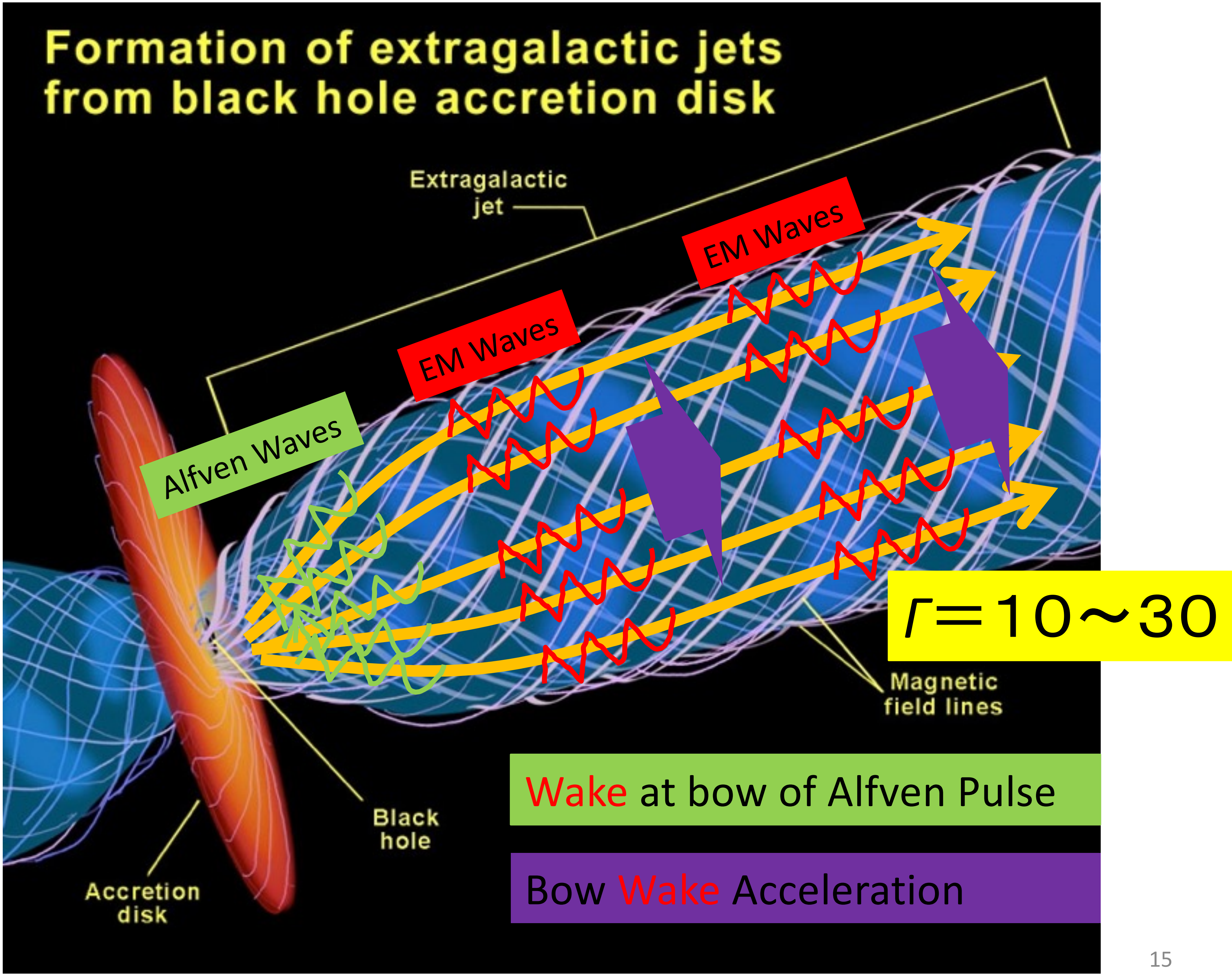

Formation of extragalactic jets from black hole accretion disk
Extragalactic jet
EM Waves
EM Waves
Alfven Waves
Γ＝10～30
Magnetic field lines
Black hole
Accretion disk
Wake at bow of Alfven Pulse
Bow Wake Acceleration

Accretion Disk around a BH

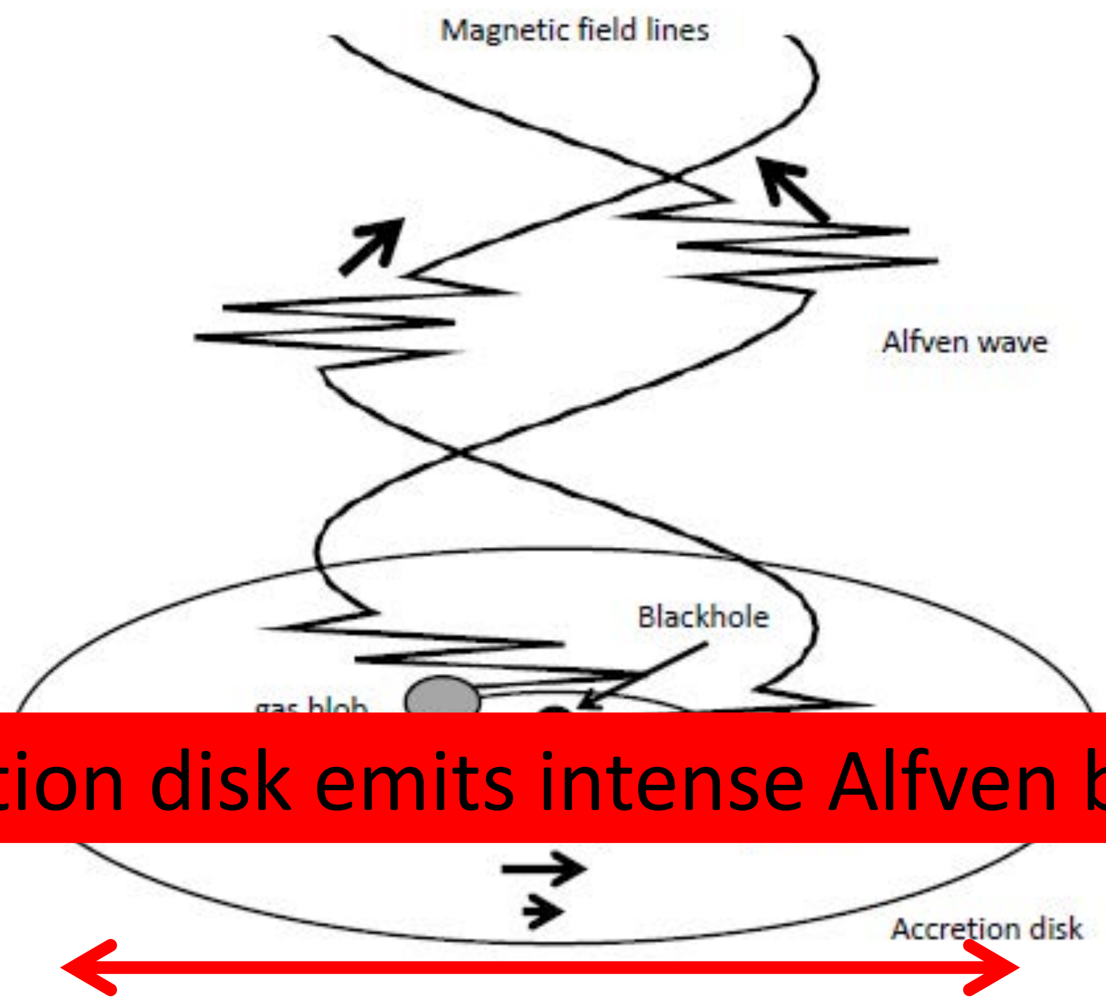

Accretion disk emits intense Alfven bursts

AGN : UHECR accelarator ?

Wakefield acceleration model (excited by Alfven wave) (Ebisuzaki & Tajima 2014)

Intense laser pulse => strong Alfven wave (v_A~c, Transverse wave)
Alfven waves excited in accretion disk propagates as outflows.

$$a = \frac{eE}{m_e \omega_A c} = 2.3 \times 10^{10} \left(\frac{\dot{M}}{0.1\dot{M}_c}\right)\left(\frac{M_{\rm BH}}{10^8 M_\odot}\right) >>1$$

nonlinear & relativistic Alfven mode Standard-disk

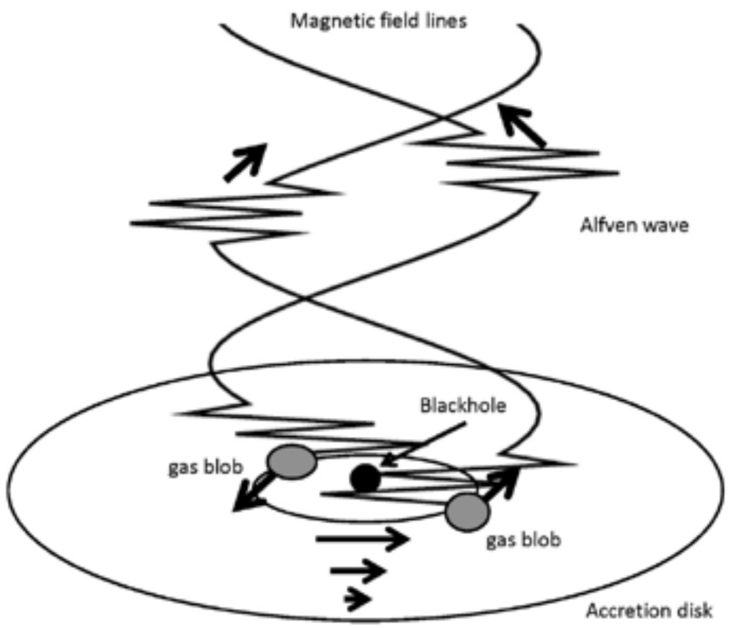

Ebisuzaki & Tajima 2014

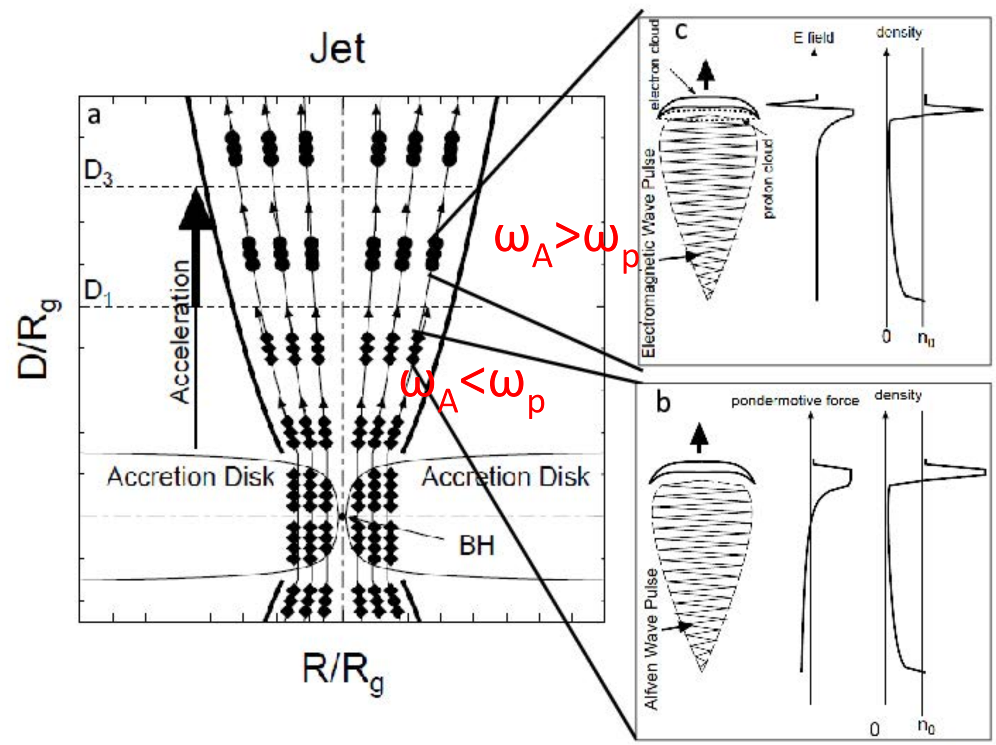

Wakefield excited on the jets from BH: genesis of EHECR and gamma bursts

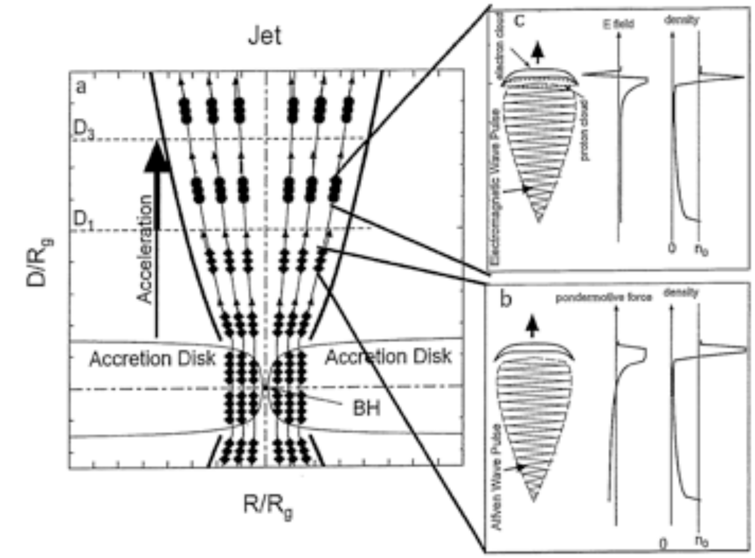

Fig. 2. (a) Schematic cross section of an disk/jet system around an accreting black hole (BH). Alfven waves (diamonds) are excited in the accretion disk and propagate along the magnetic field (thin solid curves) in the relativistic jet (thick solid curves). (b) In the pondermotive region ($\omega_c' > \omega_p' > \omega_A$), the pondermotive force of the intense Alfven wave pulse produces a bubble and accelerates particles. (c) The Alfven waves turn into electromagnetic waves (circles) as ω_A approaches and exceeds ω_p' and excites the accelerating structure whose pondermotive force fields accelecate charged particles longitudinally along the jet. We anticipate that in the extremely large a, the domain of wakefield acceleration is dwarfed by that of pondermotive acceleration in the 1D situation. In 2–3D, wakefield acceleration takes a greater role than in 1D.

Gamma emission luminosity by wakefield

$L\gamma \sim 10^{33}$ $(\kappa / 0.1)\ \eta\ m'\ m$ (erg /s)

κ (efficiency), η (episode dependent ~1)

(Ebisuzaki, Tajima, Astropart. Phy., 2014)

strong pondermotive force. Eq. 25 holds as far as Z_{acc} is greater than D. The distance D_3 is where the acceleration finishes, defined by the equation

$$D_3 = Z_{pd} = ac/\omega_A. \quad (28)$$

We find that particles arrive at D_1 before D_3, in other words:

$$D_3/3R_g = 3.9 \times 10^{3}(\dot{m}/0.1)^{5/3}(m/10^{8})^{1/3} > D_1/3R_g. \quad (29)$$

The energy spectrum of the accelerated charged particles has the power-law with the index of −2 in the 1-D model due to the multiple dephasing occurrences when particles ride on and off different peaks of the pondermotive or wakefield hills when the waves contain multiple frequencies (but with again the same phase velocity ~ c; [8]), i.e., $f(W) = A(W/W_{min})^{-2}$. As noted earlier, when the driving Alfven waves and their driven pondermotive fields hold a broad band of frequencies, their phase velocities and group velocities, respectively, are again close to the speed of light, providing the basis for the robust accelerating structure. When Alfven waves have two or three dimensional features, the dephasing is more prompt, leading to higher index of the spectrum (less than −2). Let κ be the energy conversion efficiency of the acceleration (including the mode convergence efficiency mentioned earlier), then $\kappa E_B = AW_{min}^2 \ln(W_{max}/W_{min})$, i.e.

$$A = 1.6 \times 10^{33}\kappa \dot{m} m^2 [W_{min}^2 \ln(W_{max}/W_{min})]^{-1}. \quad (30)$$

The recurrence rate ν_A of the Alfven pulse burst is evaluated as:

$$\nu_A = \eta V_{AD}/Z_D = 1.0 \times 10^{2} \eta m^{-1}\ \mathrm{Hz}, \quad (31)$$

where η is episode-dependent, and on the order of unity. This is consistent with the 3-dimensional simulations conducted by O'Neill [12]. They found magnetic fluctuations, called Long Period Quasi Periodic Oscillations (LPQPO) with the period 10–20 times the Kepler rotation period. The luminosity L_{UHECR} of ultra-high energy cosmic rays is:

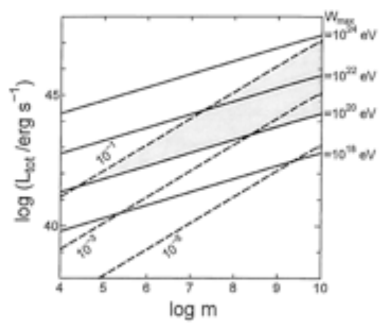

Fig. 4. The total luminosities of accreting blackholes are plotted against the blackhole mass (in the unit of solar mass) for various maximum attainable energy W_{max} (solid lines) for the case of $\Gamma = 20$ and $\xi = 10^{-3}$. Dashed lines are drawn for the values $\dot{m} = 10^{-5}, 10^{-3}$, and 10^{-1}. The grey triangle represents the parameter sets which allow the acceleration of UHECRs ($\geq 10^{20}$ eV). We set the upper limit of $\dot{m}$ to be around 0.1 for the pondermotive/wakefield acceleration to work, since the accretion disk becomes radiation dominant as $\dot{m}$ approaches unity, and the Alfven wave pulse becomes weaker than the estimate in the present paper.

4. Astrophysical implications and blazar characteristics

Radio galaxies belong to one category of AGN, which has radio lobes connected to the nucleus by relativistic jets. Their central engines are accreting supermassive ($m = 10^{6} - 10^{10}$) blackholes. Urry and Padovani [27] pointed out that there are parent (or misaligned)

Energy Flow and Spectra

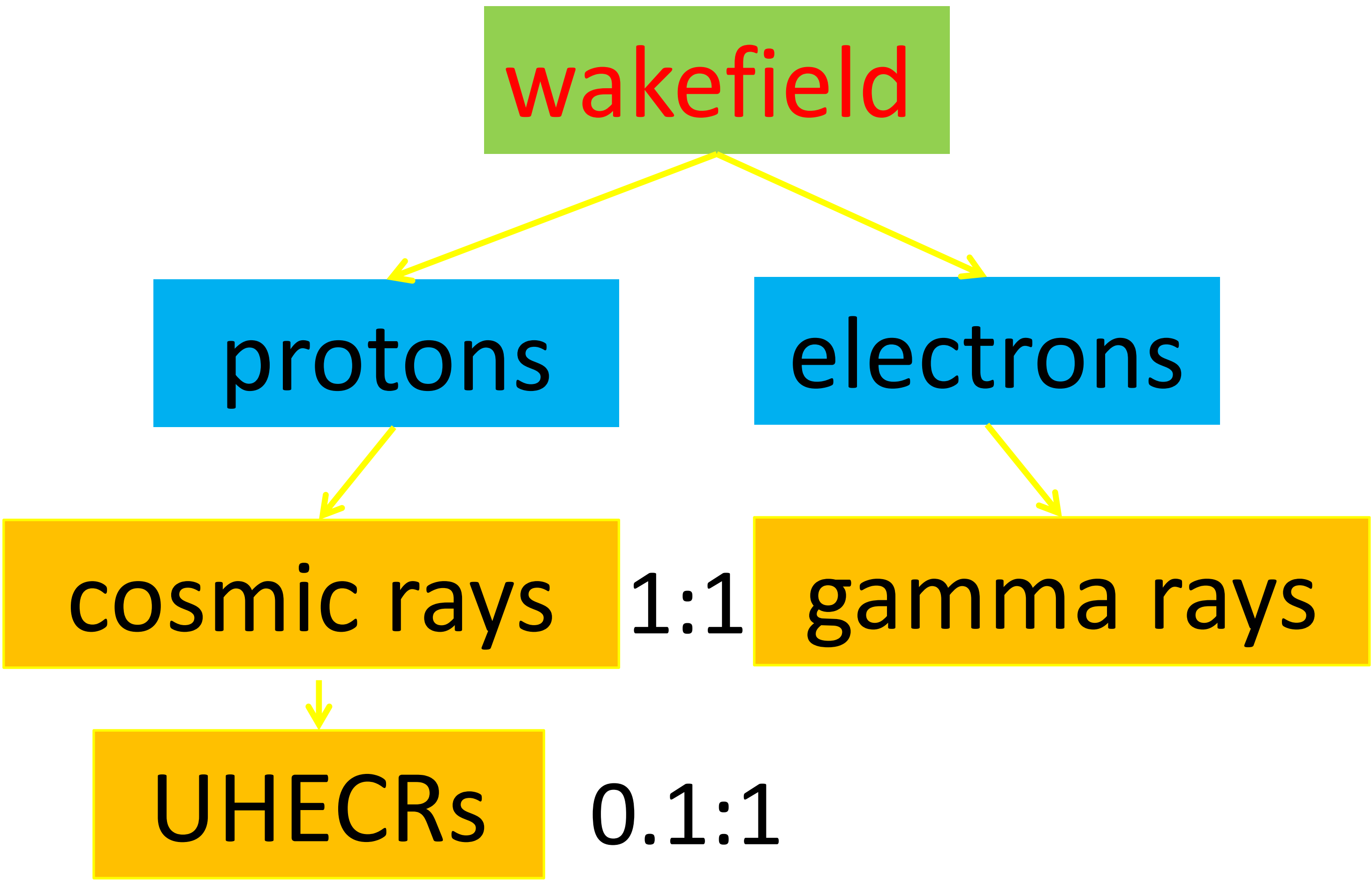

$$F(W) \propto W^{-2}$$

Anti-correlation between
Luminosity and **Power index** from **Blazars**

Anti-correlation of
Luminosity *L* of **gamma-ray** and
Power index ***p*** in time

Power index ***p*** vs.
Luminosity ***L*** for several
Blazars (more in **Abazajian** et al. arXiv **2018**)

↑

Wakefield theory anticipated(Ebisuzaki-Tajima 2014)

Blazar Variability from Wakefield Phenomena 5

L

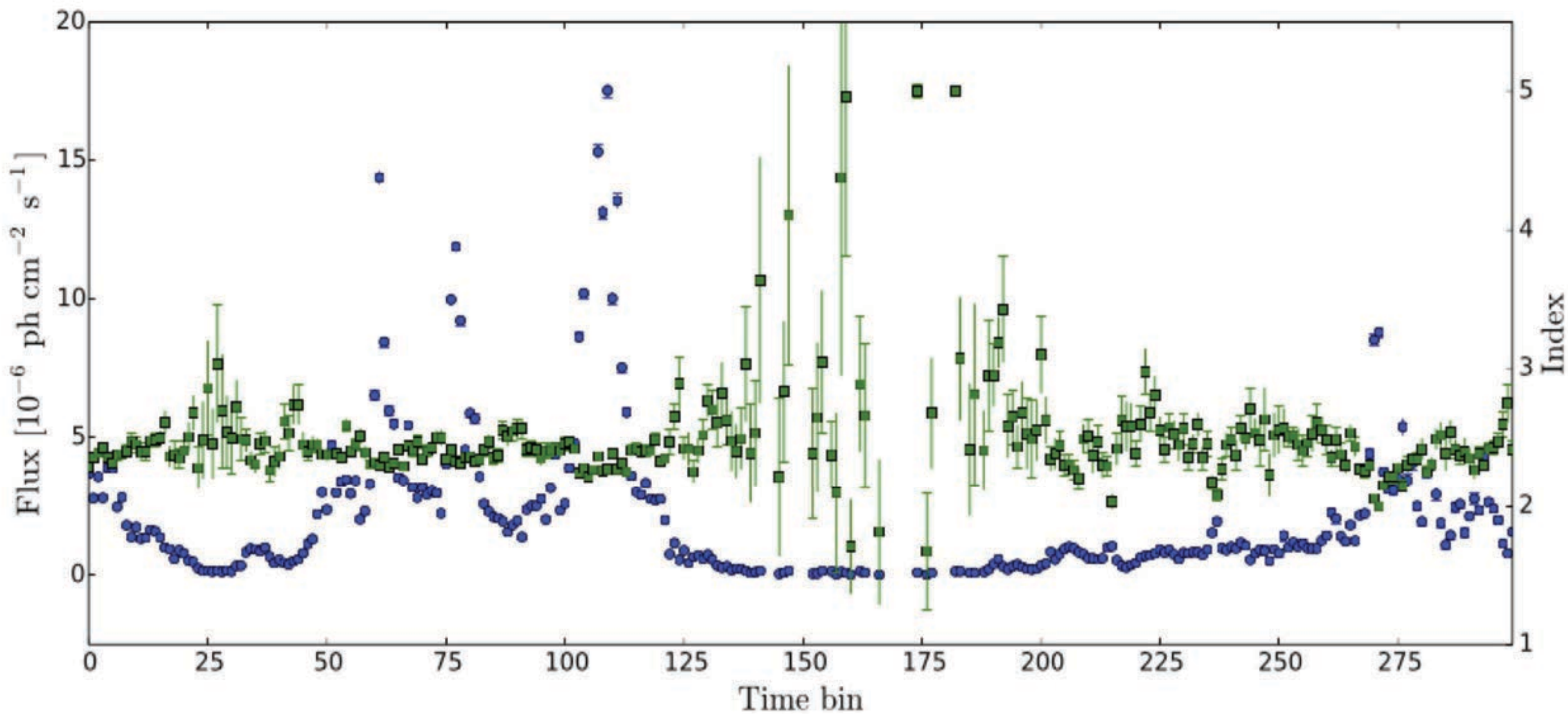

p

← ***p*=2**

Luminosity of gamma ray emission and spectrum
AGN 3C454.3 with M = 10^7 $M_\odot$

Strong accretion
→ strong wakefield

Luminosity *L*

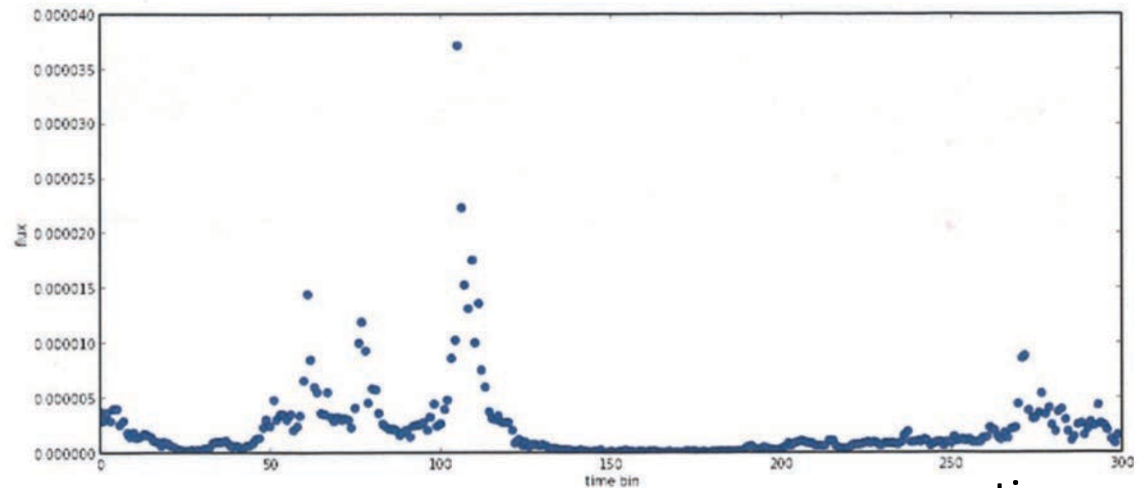

time

Spec. Index *p*

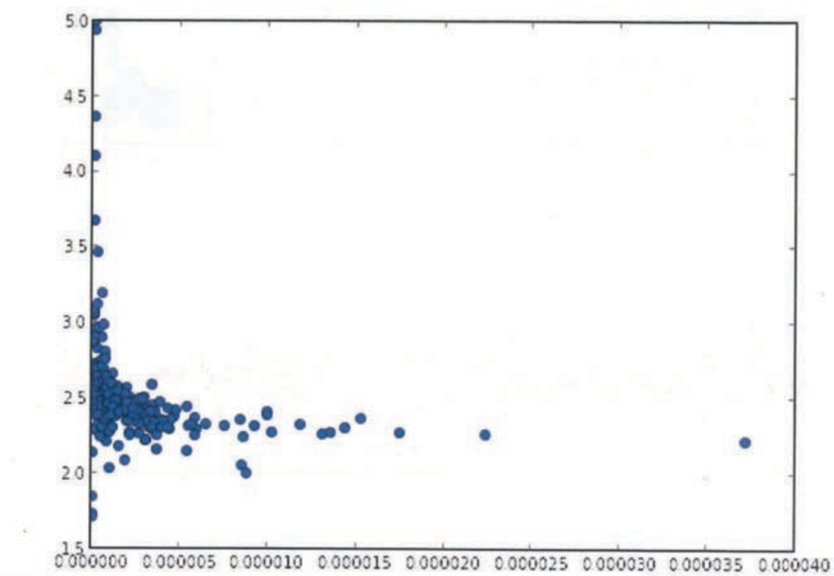

←*p=2*

Luminosity *L*

Ideal episode for wakefield:
index *p = 2,*
Otherwise *p > 2*
(Mima et al. 1991; Takahashi, Hillman,Tajima, 2000, Ebisuzaki et al. 2014)

Gravitational wave and Gamma bursts

Fermi satellite x LIGO

- gamma bursts →
- GW synchronize precedes gamma bursts

see (Ebisuzaki et al, 2014)
Neutron star-Neutron star collision
→ similar wakefields
(Takahashi et al. 2000)

Simulataneous **Gravitational Waves****
(Barish**'s talk at UCI, 2018) →

**) Nobel in Physics (2017)

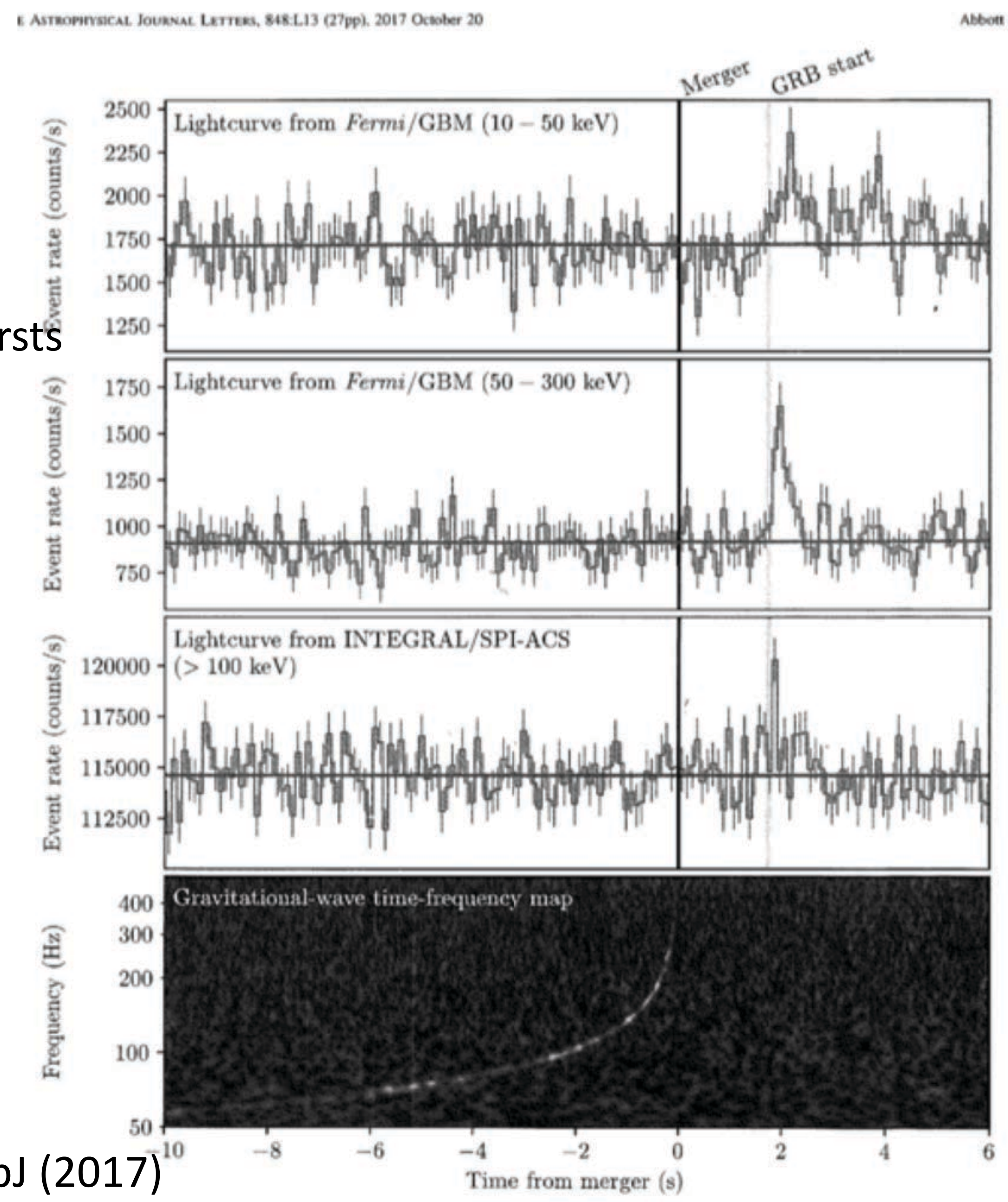

Abbott et al. ApJ (2017)

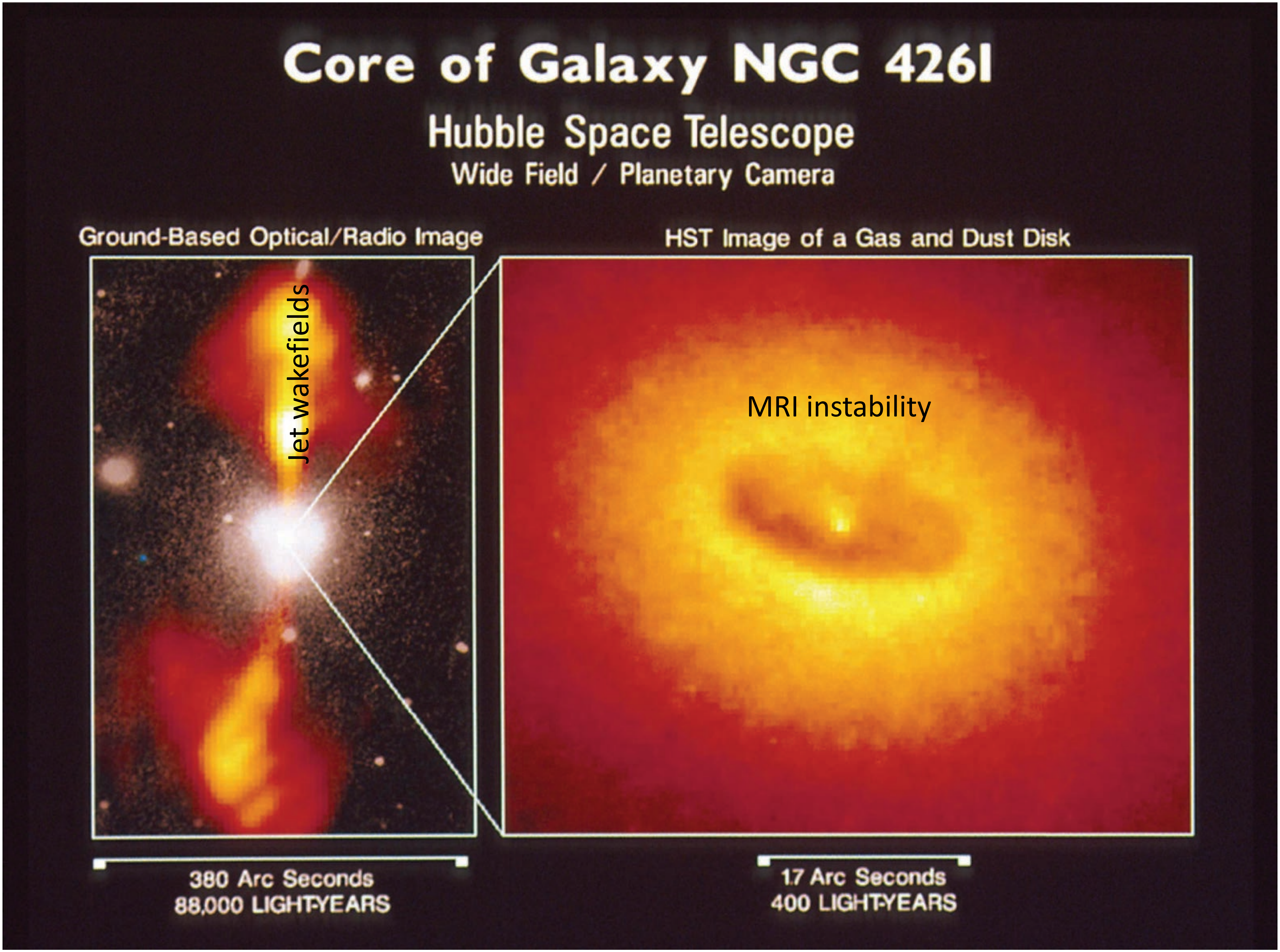
Core of Galaxy NGC 4261
Hubble Space Telescope
Wide Field / Planetary Camera
Ground-Based Optical/Radio Image
HST Image of a Gas and Dust Disk
Jet wakefields
MRI instability
380 Arc Seconds
88,000 LIGHT-YEARS
1.7 Arc Seconds
400 LIGHT-YEARS

High Energy Neutrino Flux (IceCube): wakefield theory

Barwick et al. (2013 preparation)

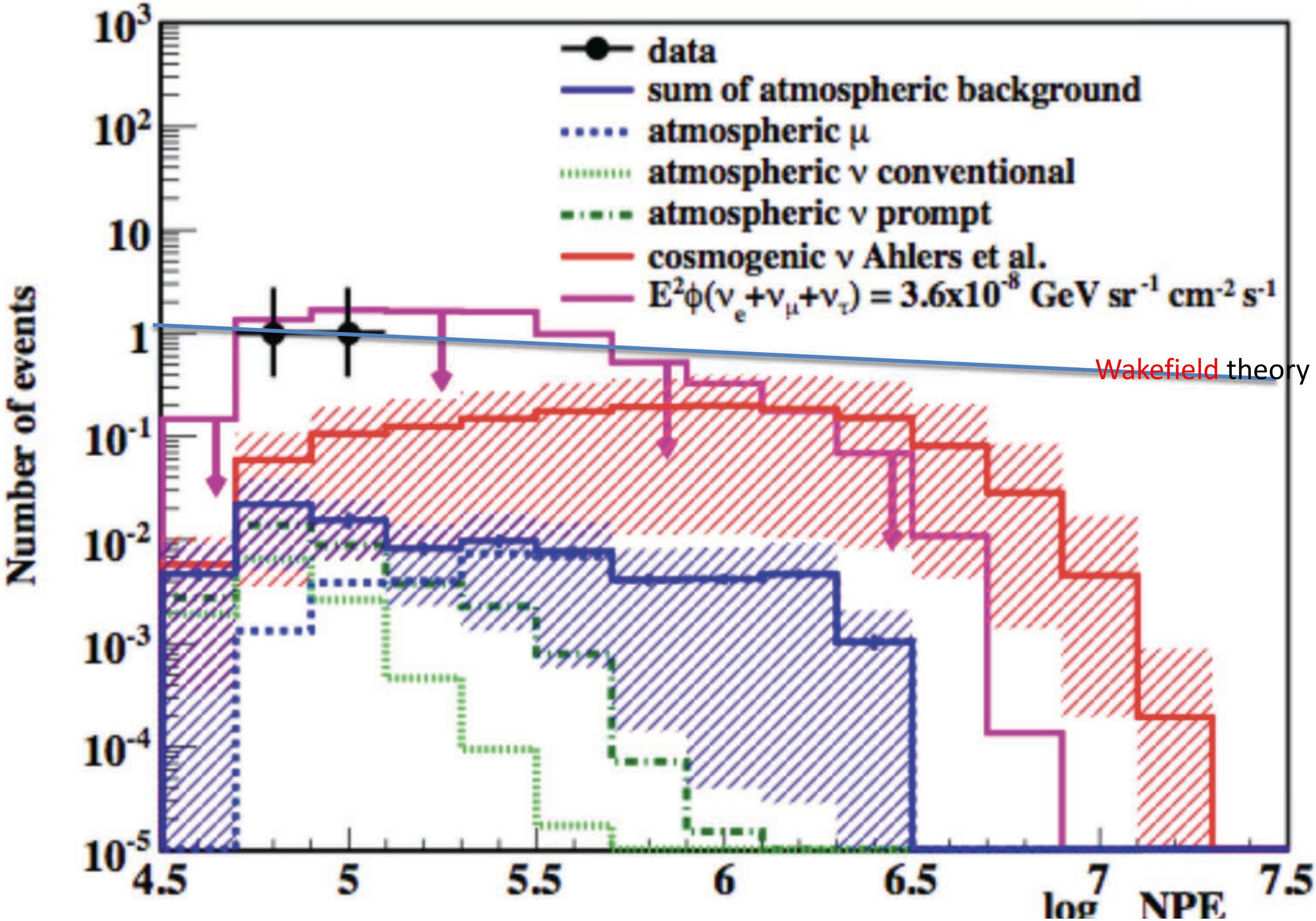

Cosmic-ray up to ~10^{20}eV

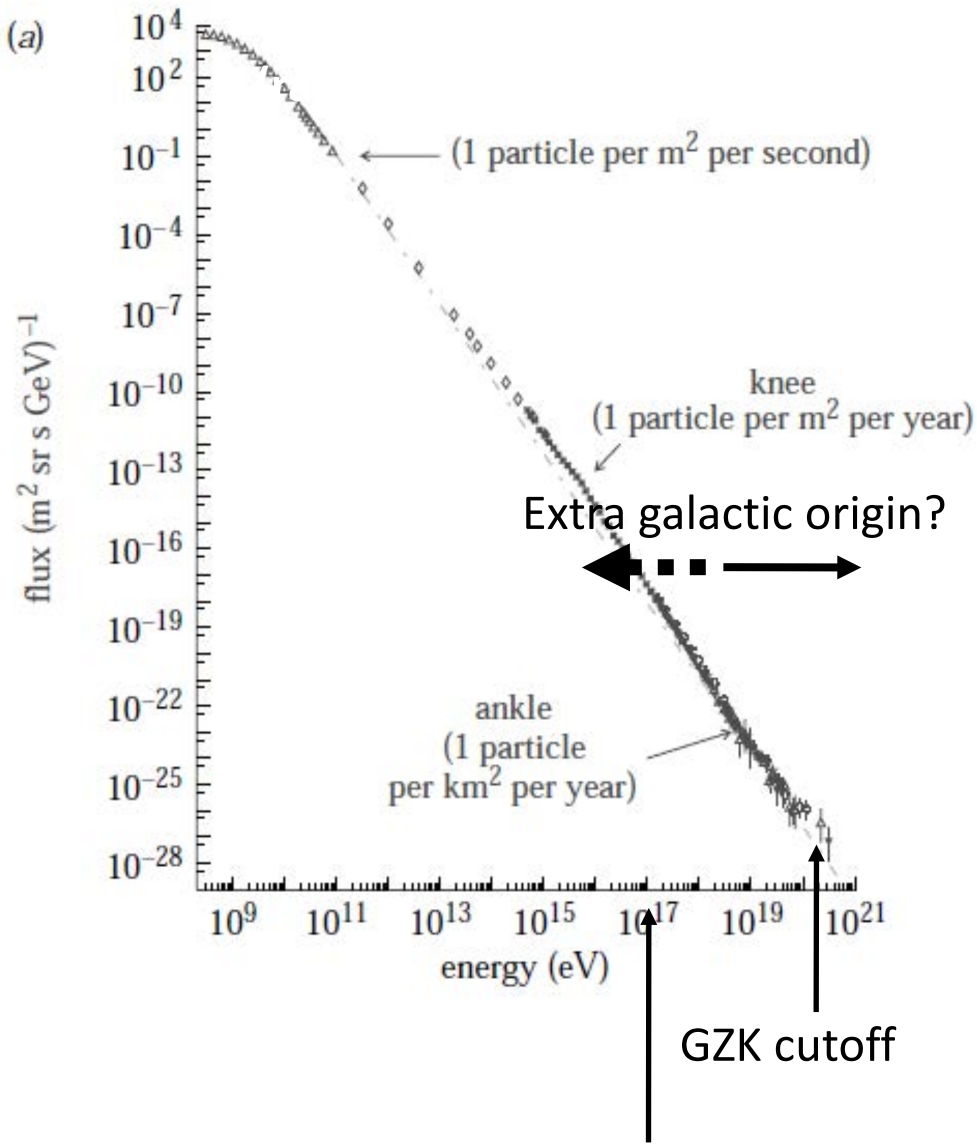

Hillas plot : E_{max}~ $ZeBR$

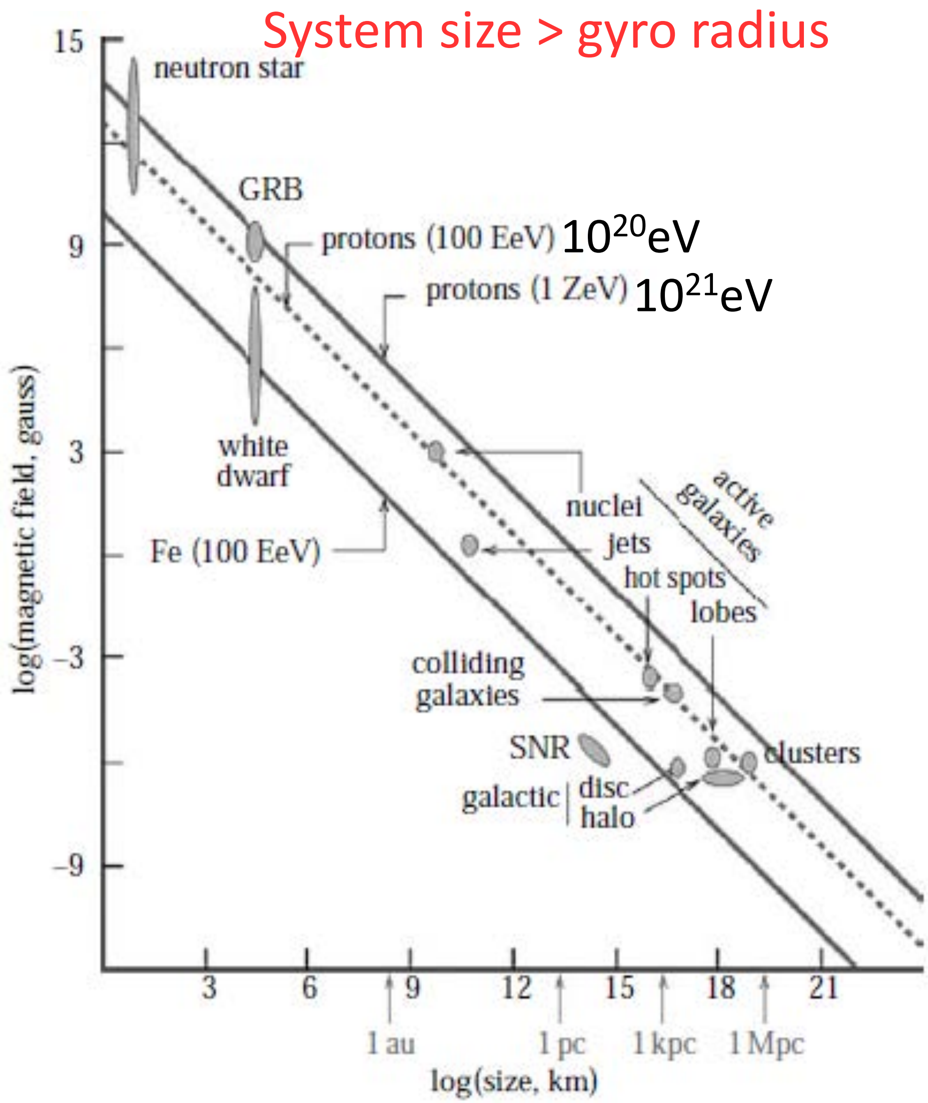

LHC(14TeV Center-of-mass system)

Cosmic-ray up to ~10^{20}eV

~10^{23}cm

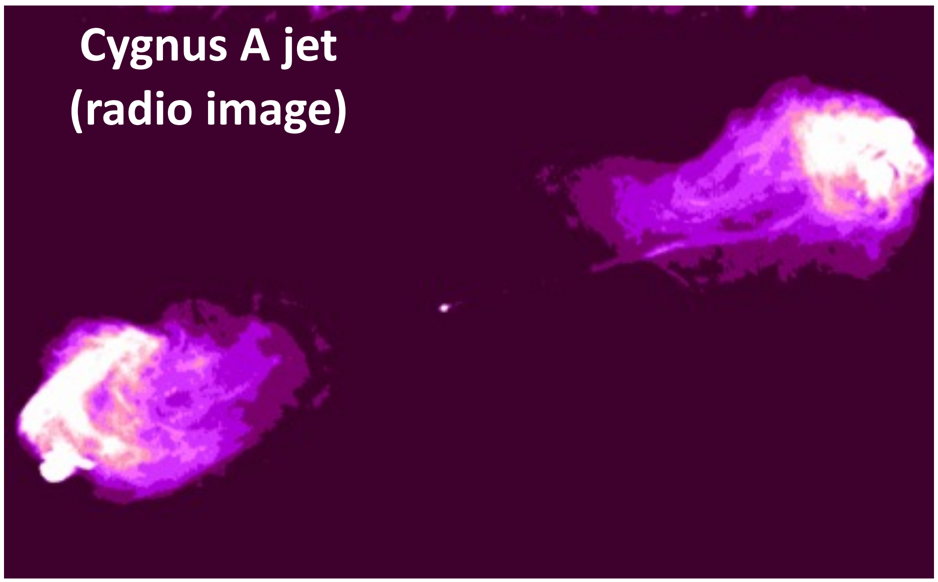

Hillas plot : Emax~ZeBR

System size > gyro radius

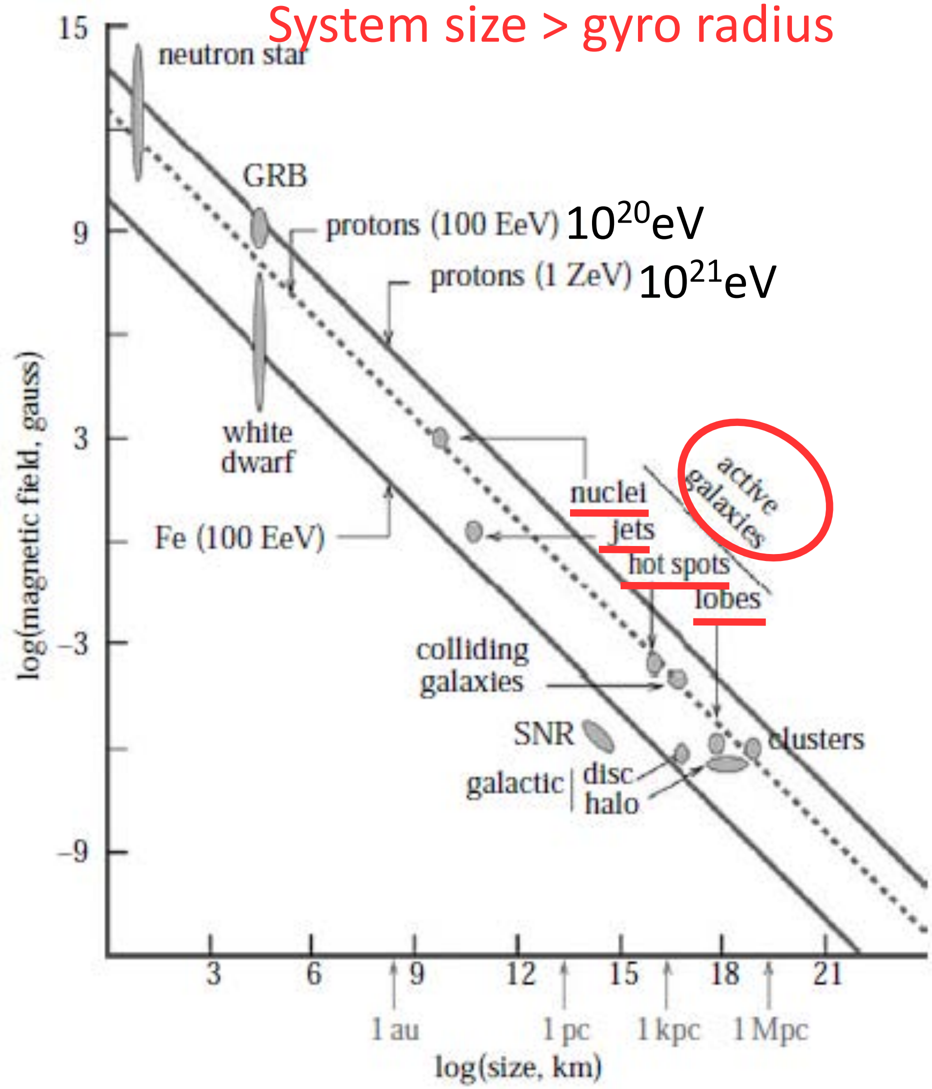

Active galactic nuclei (AGN) jets are one of strong candidate objects for UHECR accelerator.

comic ray acceleration and gamma-ray emission

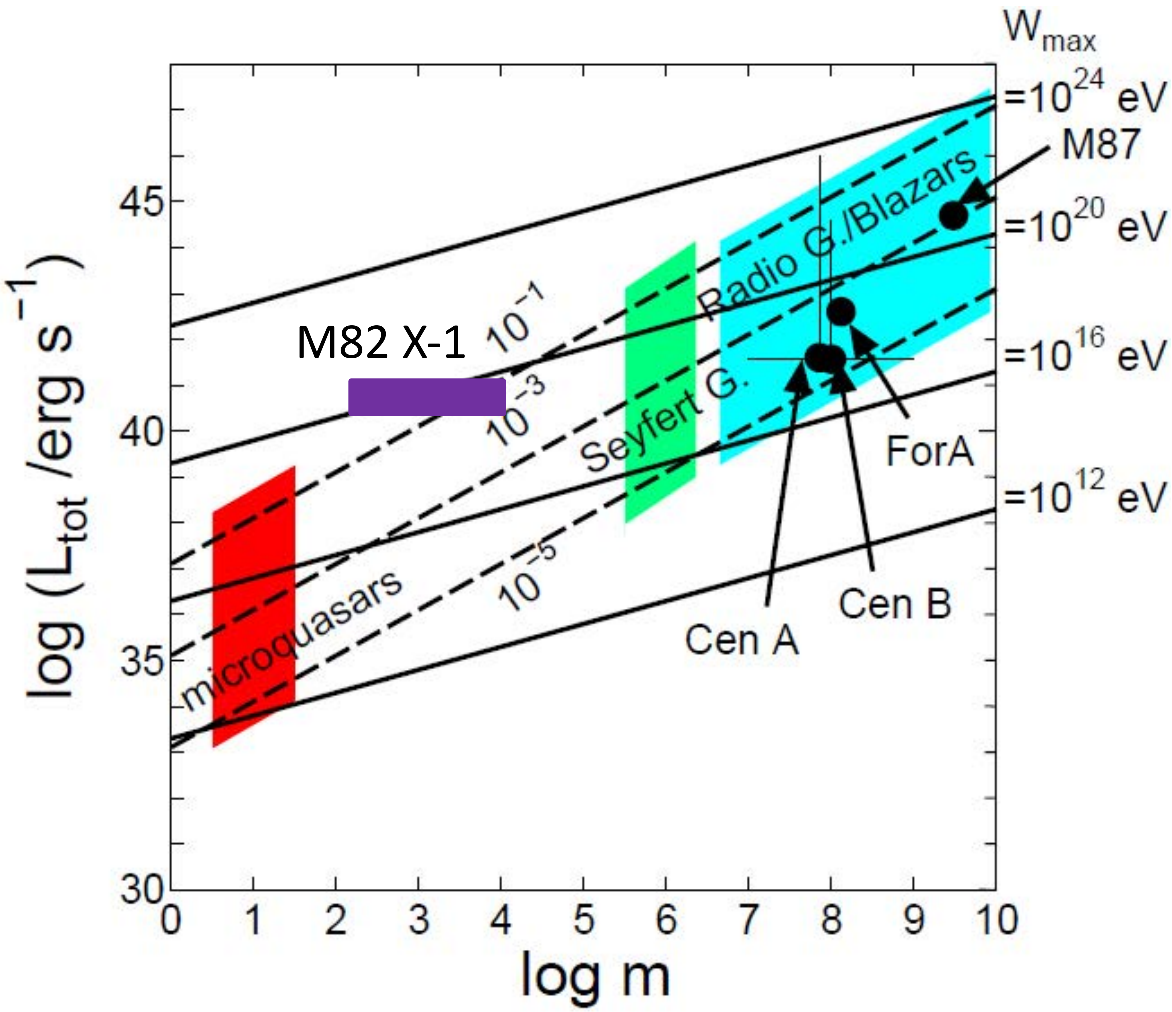

$$L_{\rm tot} = 1.3{\times}10^{38} m\dot{m}\ \ {\rm erg\,s^{-1}}$$

MRI drives wakefields

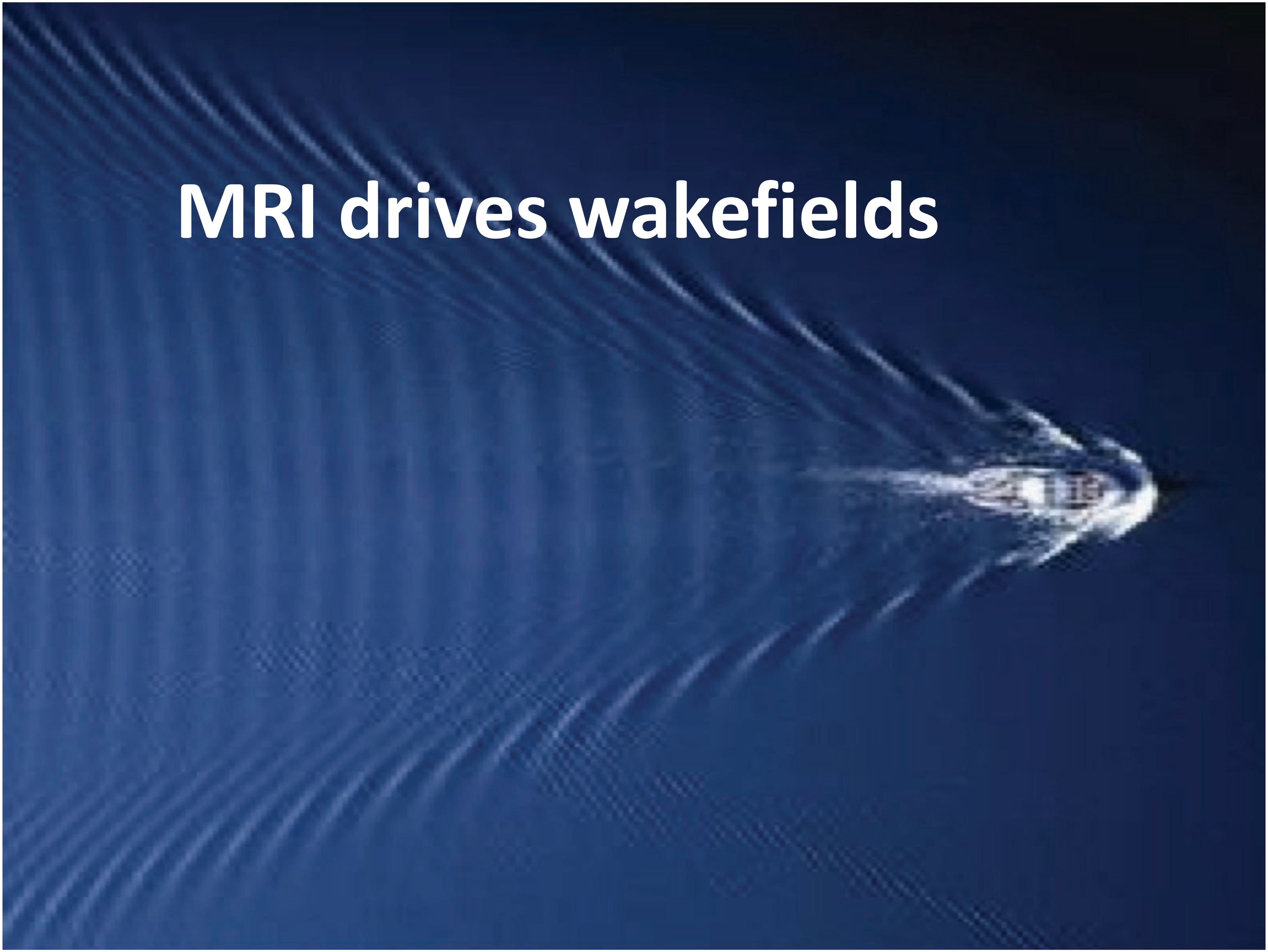

Blazars in the Model of AGN

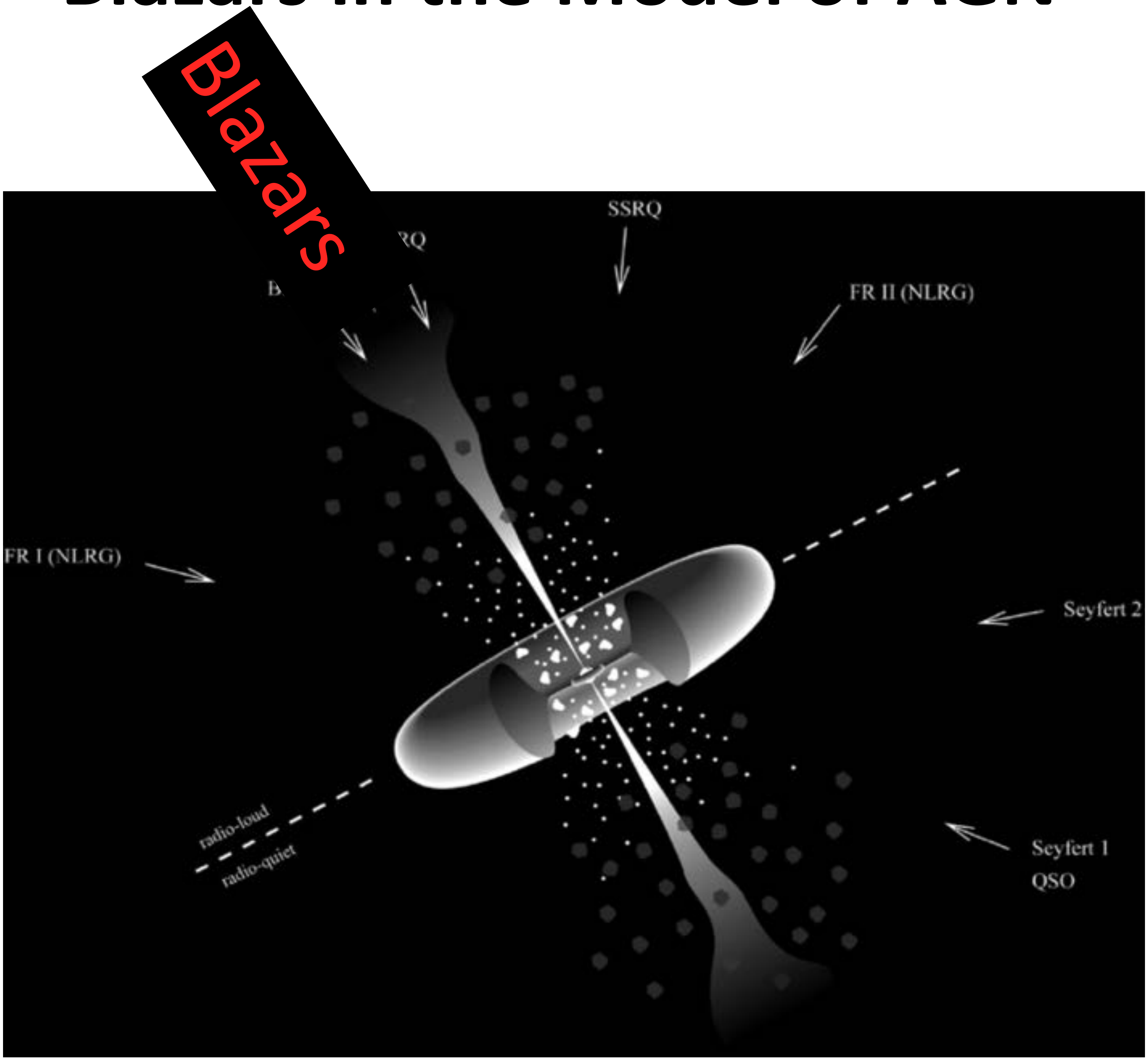

Blazars Flares From Accretion Disk

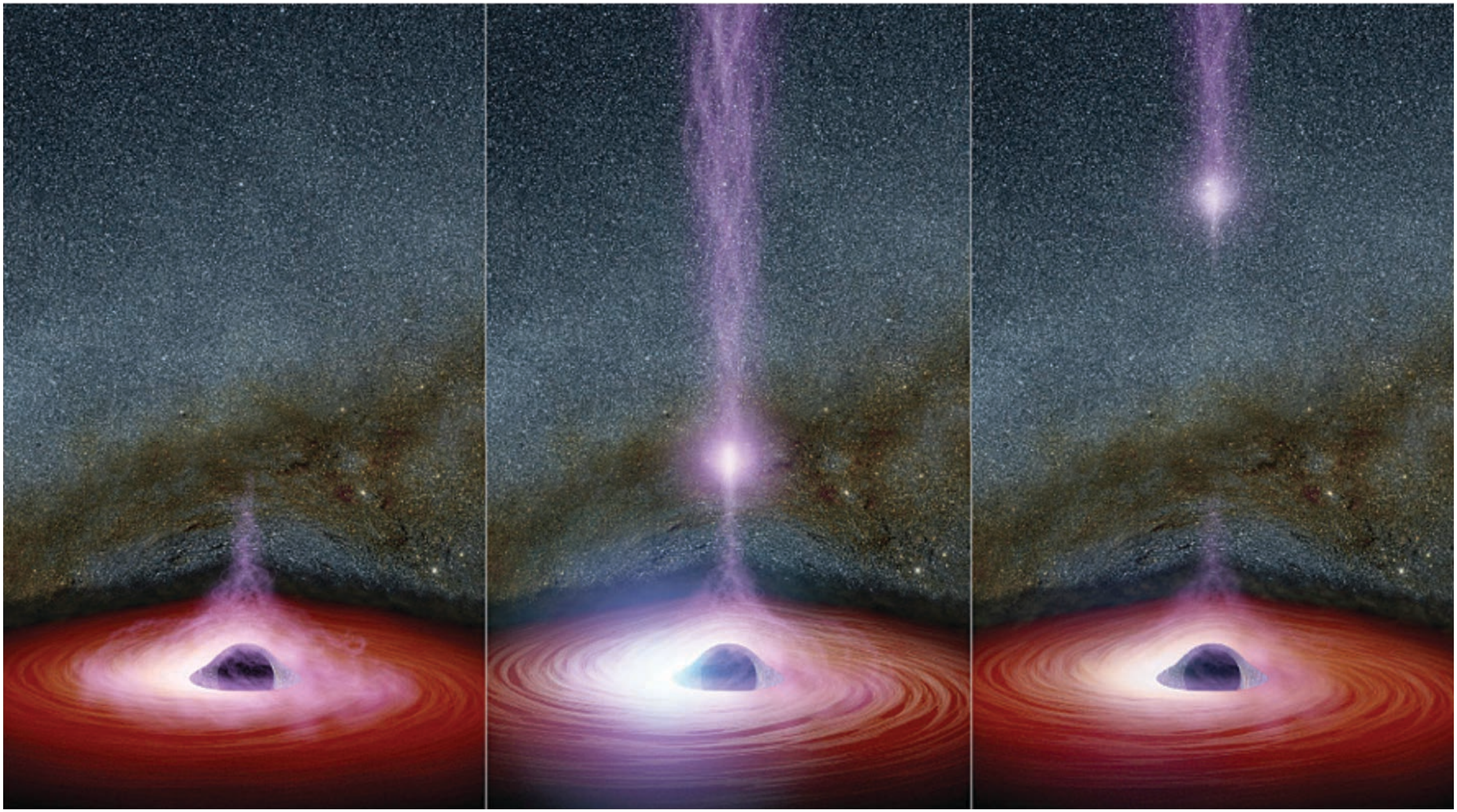

Launching magnetized relativistic jets and cosmic ray acceleration by wakefield acceleration triggered by strong Alfvenic wave.

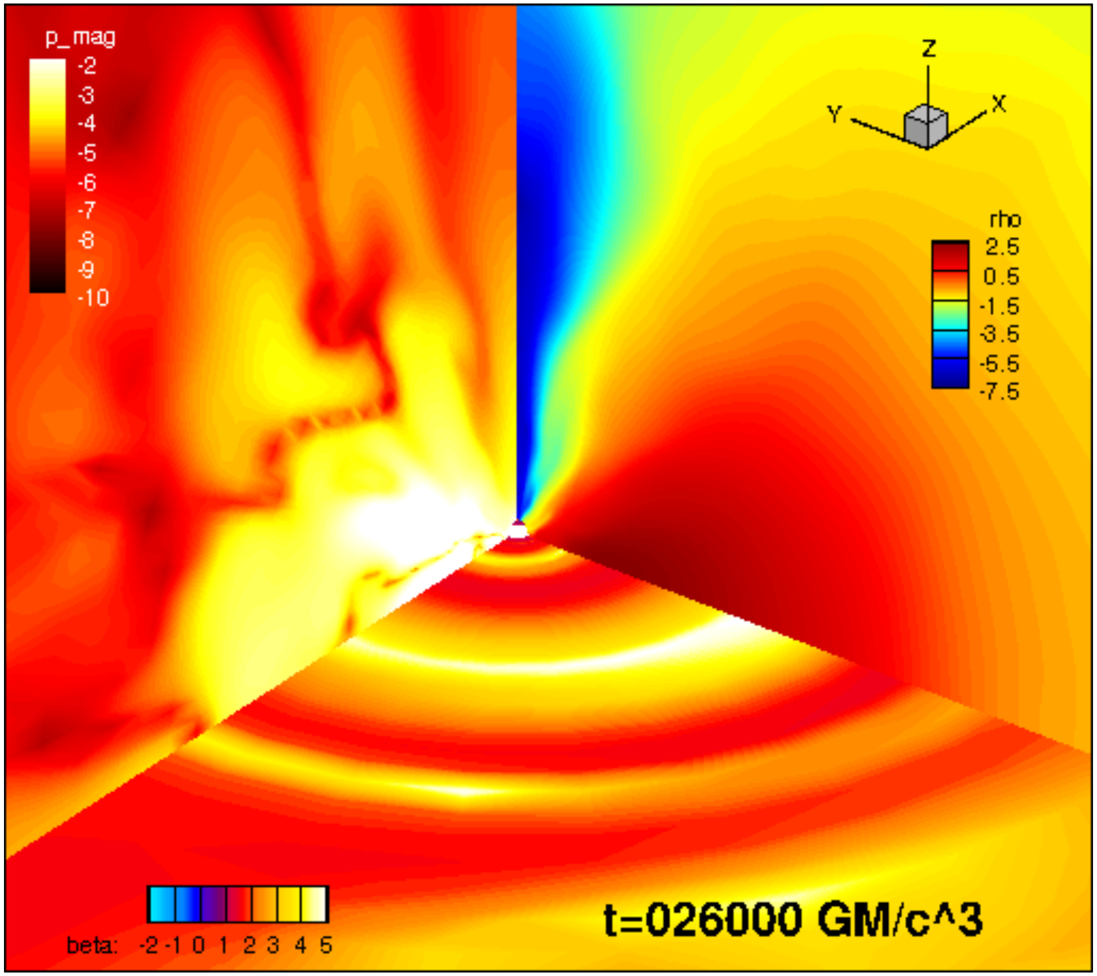

Akira MIZUTA(RIKEN)

Outlook on Wakefield
Acceleration: the Next Frontier
15 Oct. 2015 @ CERN

Magnetized jet launch

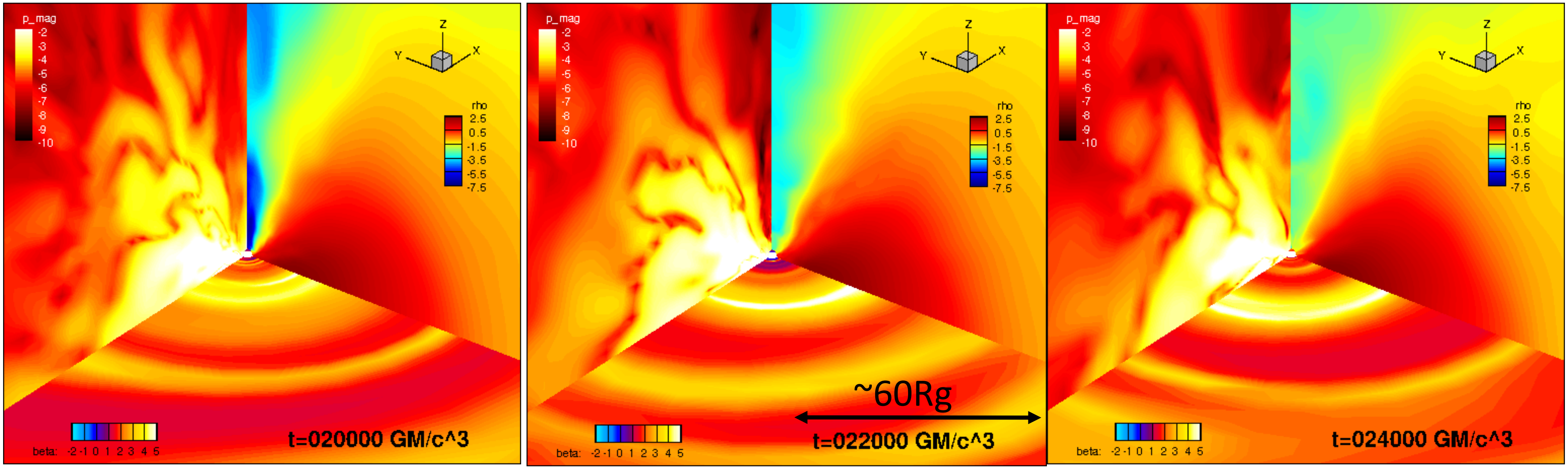

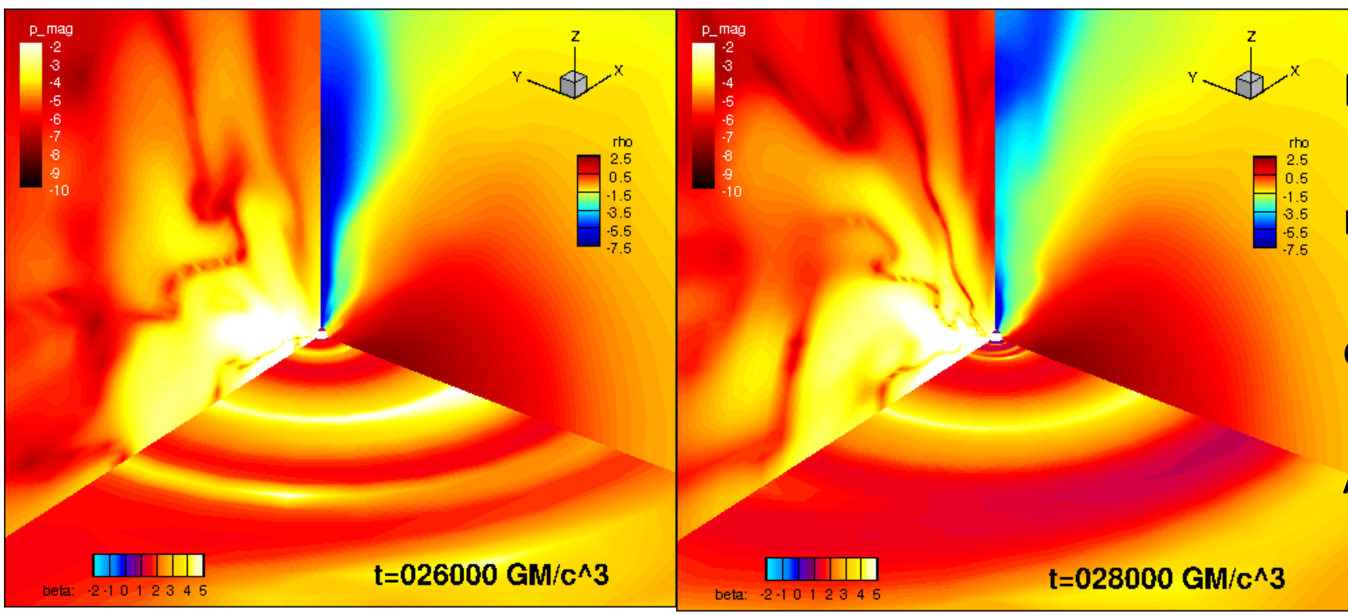

DISK

- Stratified structure in magnetic energy density
- Disk wind along the disk edge

Along the polar axis

- Mass density is low
- intermittent outflow
- High Magnetic energy density

History of accretion rate r=1.4R_g (@horizon)

$$M_{\rm dot} = \int_{\theta=\theta_0}^{\theta=\theta^1} \int_{\phi=0}^{\phi=2\pi} \sqrt{-g}\rho u^1 dA$$

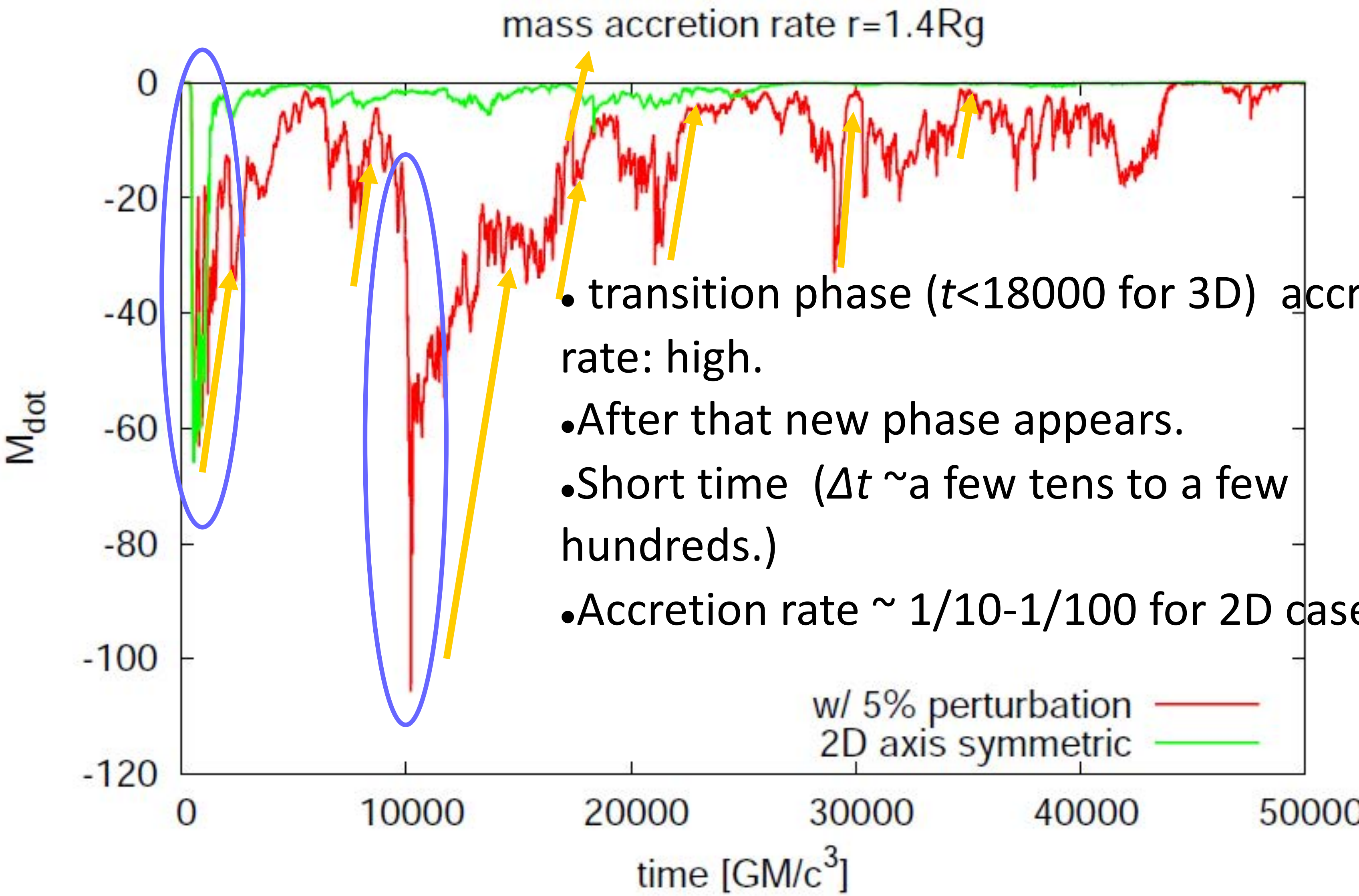

- transition phase (t<18000 for 3D) accretion rate: high.
- After that new phase appears.
- Short time (Δt ~a few tens to a few hundreds.)
- Accretion rate ~ 1/10-1/100 for 2D cases.

B-field amplification, saturation, and dissipation

$$E_{\rm EM} = -\int_{r=r_0}^{r=r_1}\int_{\theta=\theta_0}^{\theta=\theta_1}\int_{\phi=0}^{\phi=2\pi}\sqrt{-g}T^{t}_{t\,\rm EM}dV$$

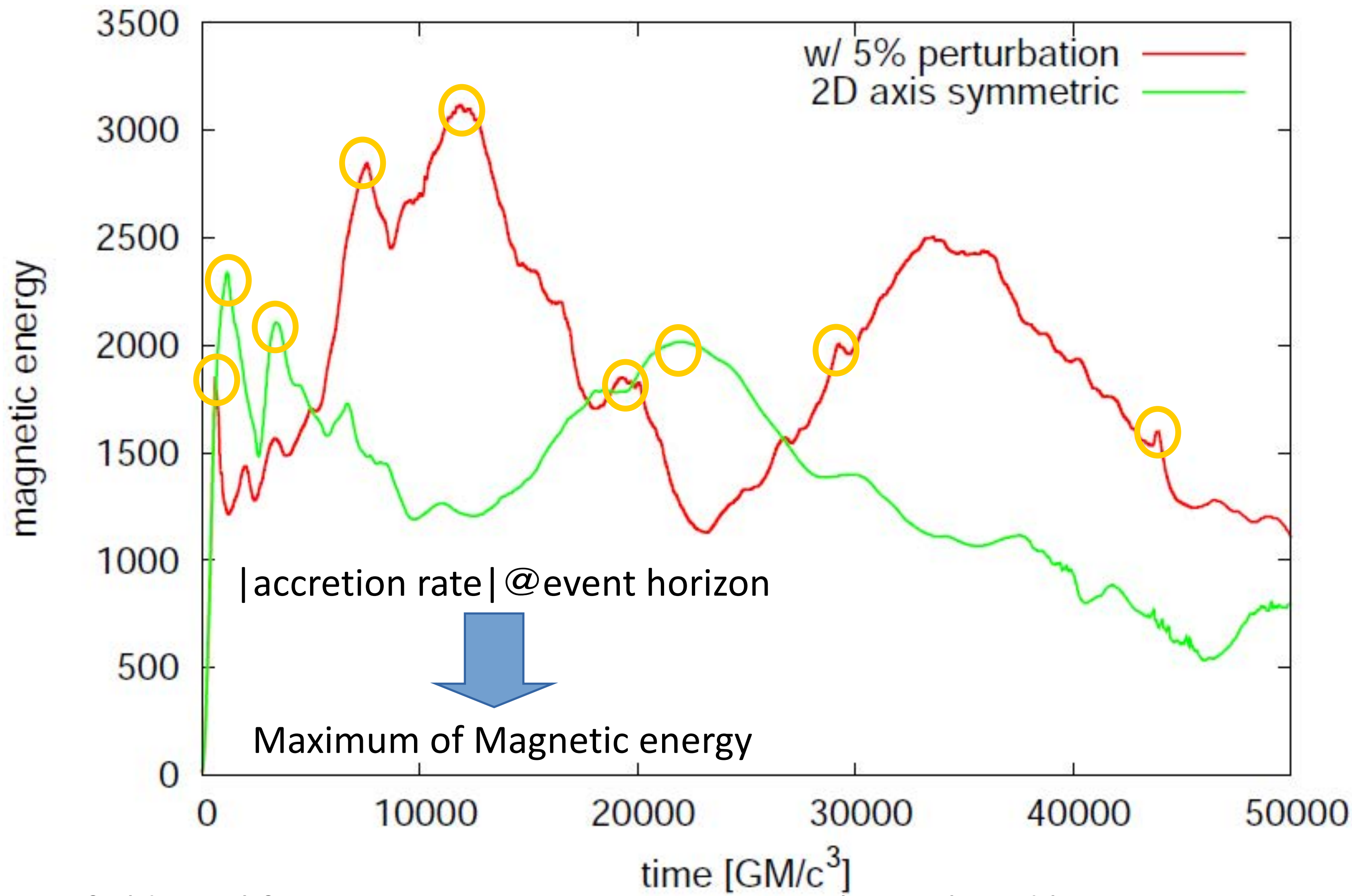

Magnetic field amplification, saturation, conversion to thermal, and kinetic energy repeat. intermittent feature for outflow.

Outflow luminosity (0 < θ < 10°)

$$E_{\rm dot} = -\int_{\theta=\theta_0}^{\theta=\theta_1}\int_{\phi=0}^{\phi=2\pi}\sqrt{-g}T^r_t\,dA$$

$\boldsymbol{\theta_0}=0$

$\theta_1=10$

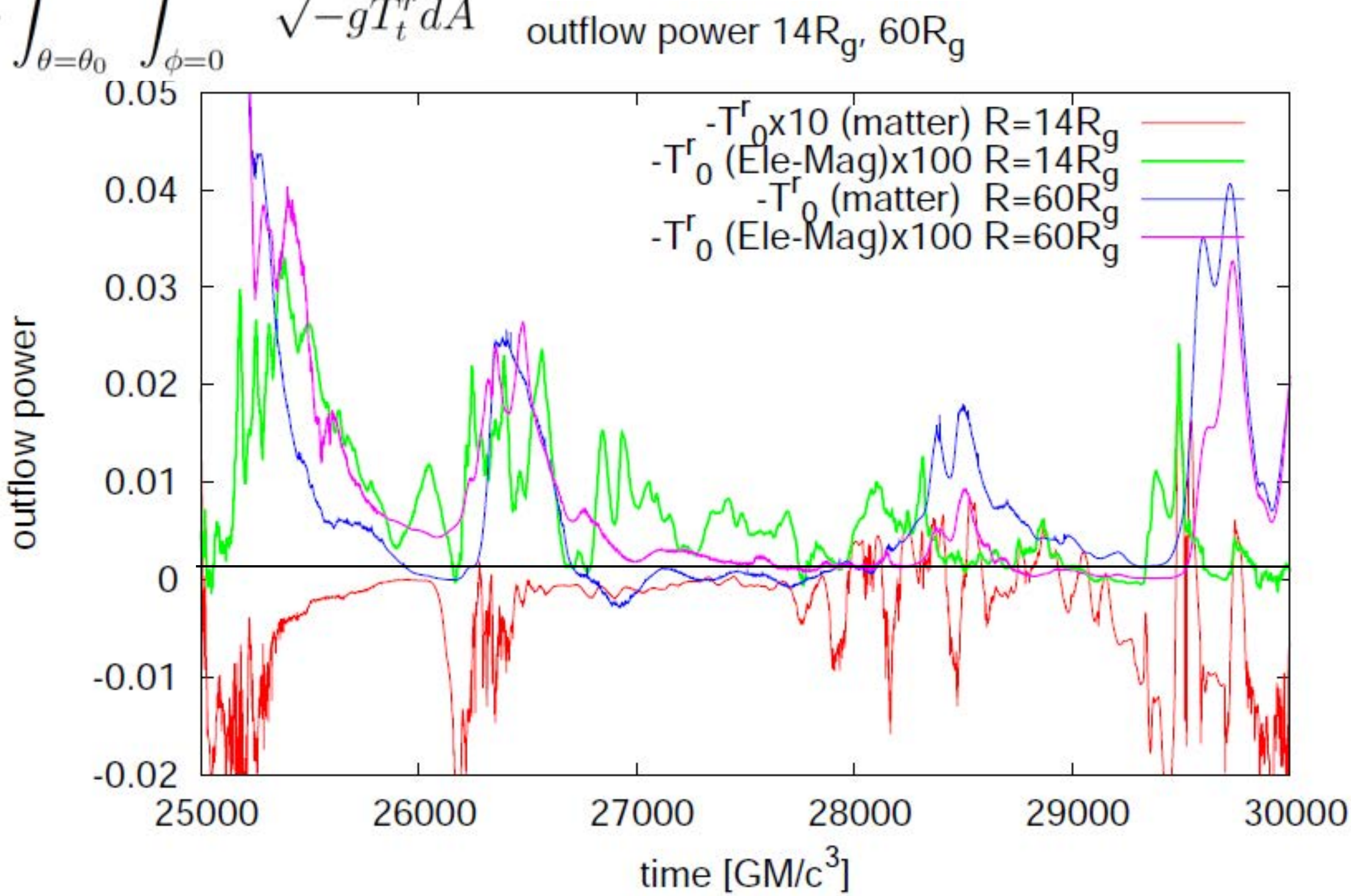

Short time variability (*Δt*~a few tens GM/c^3) in EM

(green and pink) : Good agreement = Ebisuzaki & Tajima(2014)

=> possible origin for blazar flares,

strong Alfven wave mode => Application to wakefield acc. for UHECRs

Enhanced energy emission of jets and wakefields by merging two NS's (or BH's)

(Takahashi, Hillman, Tajima, 2000)

in <u>High Field Science</u>, Eds., T. Tajima, K., Mima, and H. Baldis (Kluwer, NY, 2000).p177.

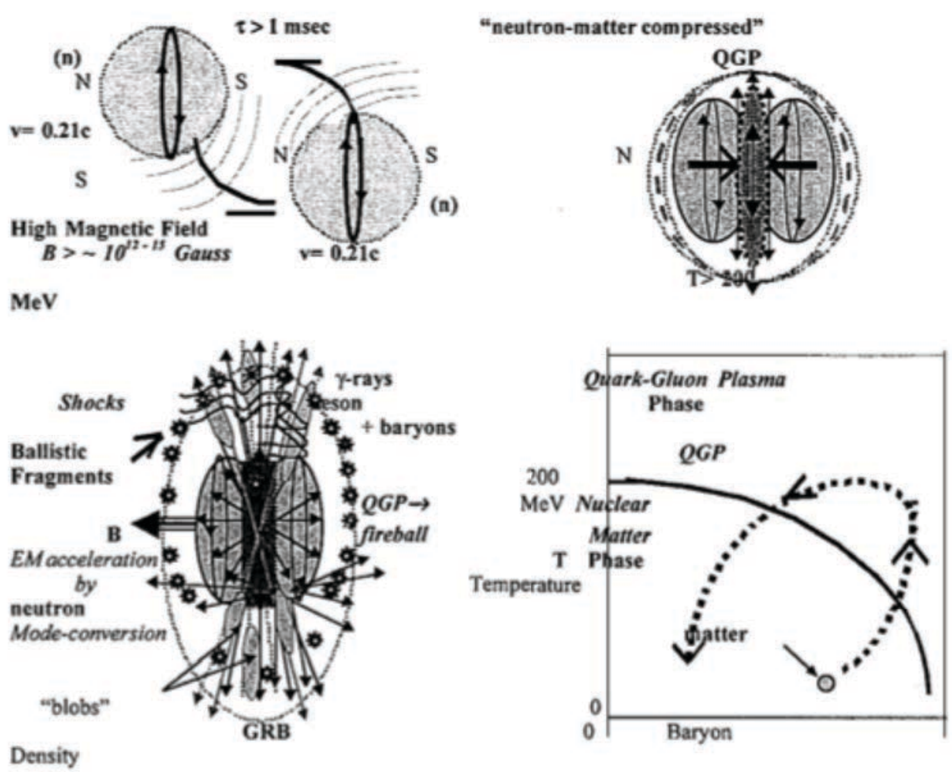

Figure 2. Schematic illustrations of QGP formation in the merge of spinning neutron stars.

GRB including high energy particles

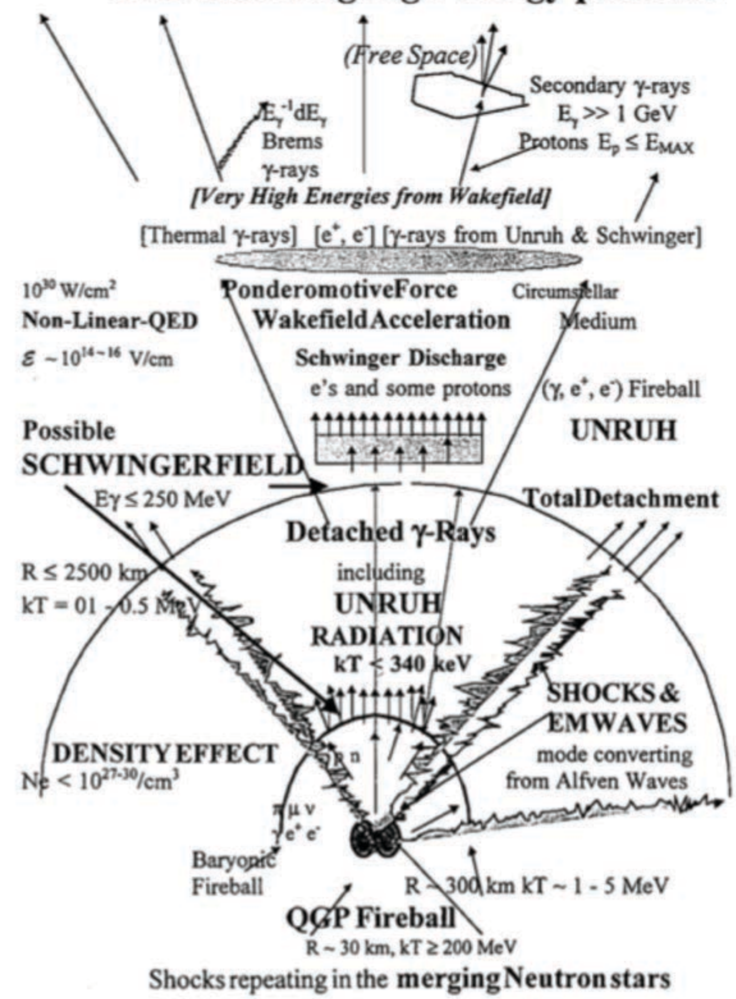

Figure 8. A schematic illustration of the proposed concept.

Also, Chen, Tajima, and Takahashi, PRL (2002).

Merging BHs and their emission of gravitational waves

Matsubayashi, Shinkai, Ebisuzaki (ApJ,2004)

Dimensionless amplitude of the gravitational wave

$h \sim 5 \times 10^{-21}\, \varepsilon^{1/2}\, R^{-1}\, \mu$

ε (efficiency normalized to 0.01),
R (distance in 4 Gpc))
μ (reduced mass of two stars in 10^3 solar mass)

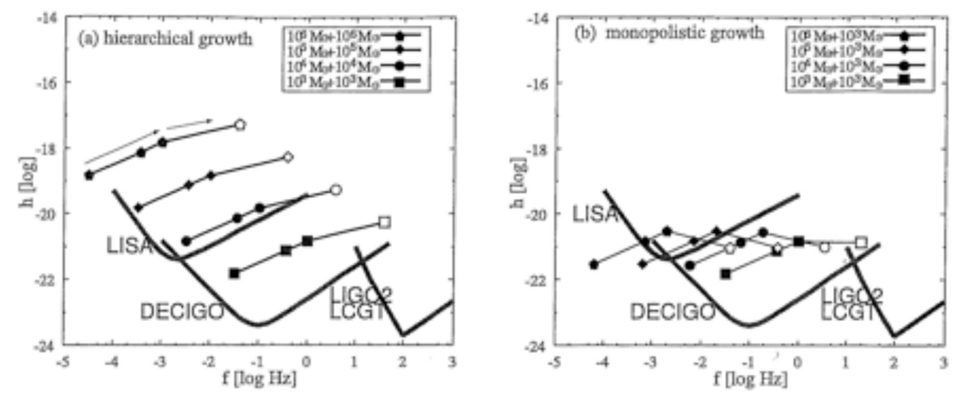

FIG. 1.—Expected gravitational radiation amplitude from merging IMBHs of (a) the hierarchical growth model and (b) the monopolistic growth model. We plot both the inspiral phase ($f_{\rm insp}$, $h_{\rm insp}$; eqs. [2] and [3]) and the ringdown phase ($f_{\rm QNM}$, $h_{\rm rad}$; eqs. [4] and [6]) for various mass combinations. The open and filled circles and squares in the inspiral phase are of $a = 50R_{\rm grav}$, $10R_{\rm grav}$, and $5R_{\rm grav}$. The final burst frequency, $f_{\rm QNM}$, depends on the efficiency, ϵ, which we fix at $\epsilon \simeq 10^{-2}$ for the plots. The lines represent the sensitivities of future detectors (LISA, DECIGO, LIGO 2, and LCGT), taken from Fig. 1 in Seto et al. (2001). The data are evaluated at the distance $R = 4$ Gpc.

Conclusions

- **Wake Acceleration: nature's** natural gift as accelerator
- Physical mechanism: robust Higgs' state; high phase velocity
- Accreting BH+disk+jets = **Astronomical Linear accelerator**
- Bursts of Intense Alfven waves ←Laser; Jet ←wave guide
- Simultaneous events: gamma ray bursts (GeV-TeV); flares; high energy cosmic rays (neutrino bursts); sometimes GW
- Gamma rays: Episodic eruptions; anti-correlation of luminosity and power index; characteristic fine structures; power-law 2 or > 2)
- Plasma: "The stronger the bang (under $v_{ph} >> v_{th}$) is, the more resilient the accelerating structure is."
- More astrophysical observations needed


Thank you!

Thin Film Compression and CAIL, and Toilet Science

Mourou* et al. (2014)

Single-cycle laser (new Thin Film Compression)

Laser power = energy / pulse lnegth

Optical nonlinearity of thin film → pulse frequency width bulge, pulse compression

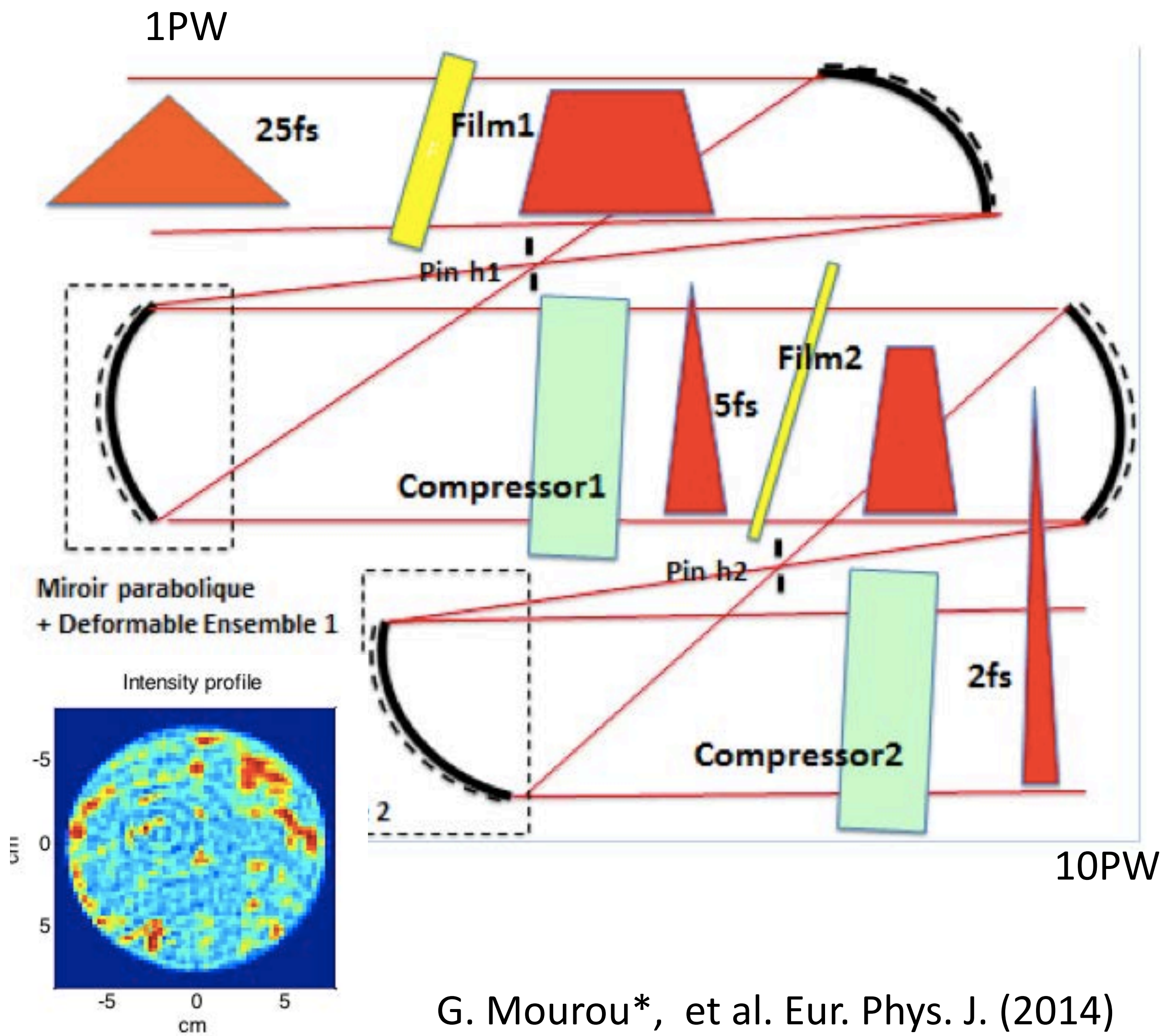

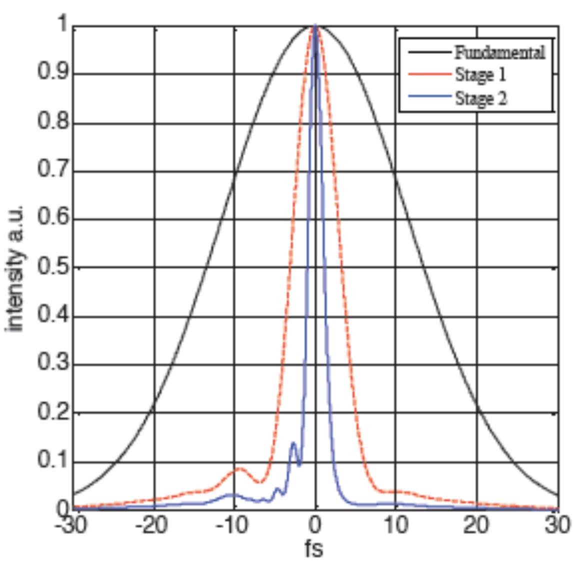

G. Mourou*, et al. Eur. Phys. J. (2014)

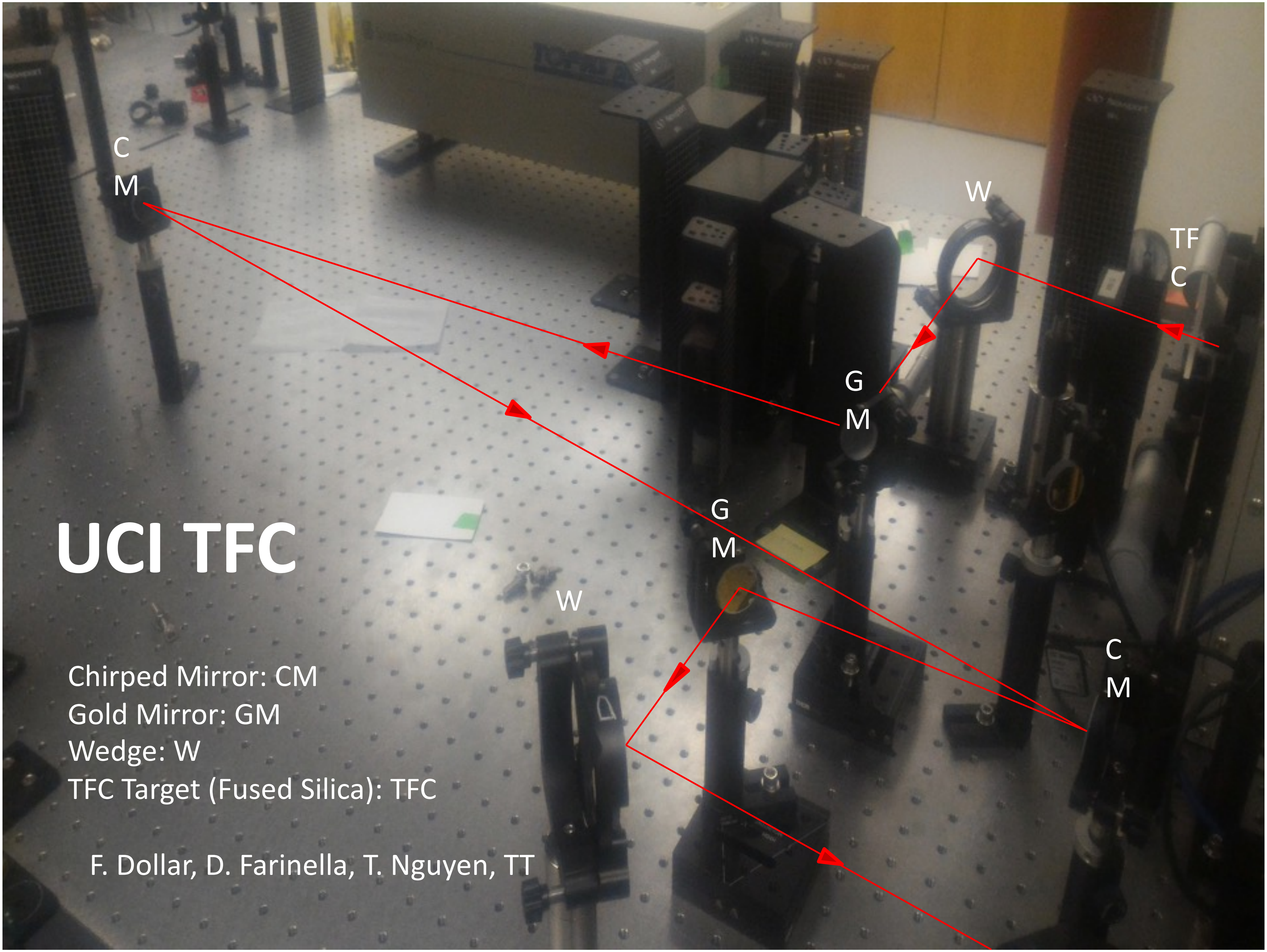

UCI TFC

Chirped Mirror: CM
Gold Mirror: GM
Wedge: W
TFC Target (Fused Silica): TFC

F. Dollar, D. Farinella, T. Nguyen, TT

Adiabatic (Gradual) Acceleration

from #1 lesson of Mako-Tajima problem (1978)

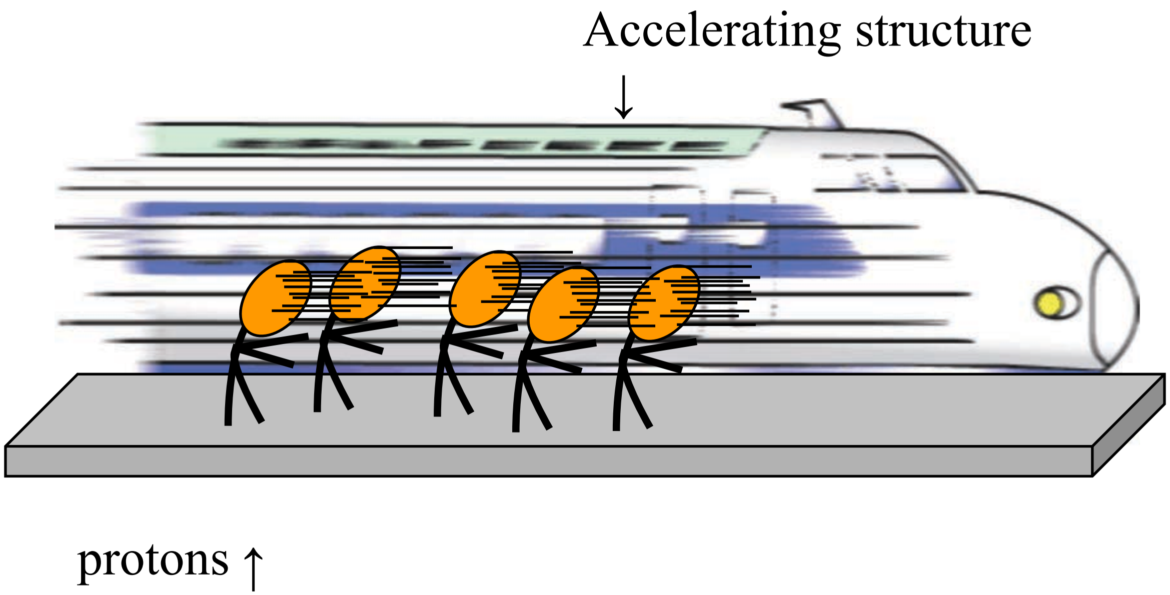

Inefficient if <u>suddenly</u> accelerated

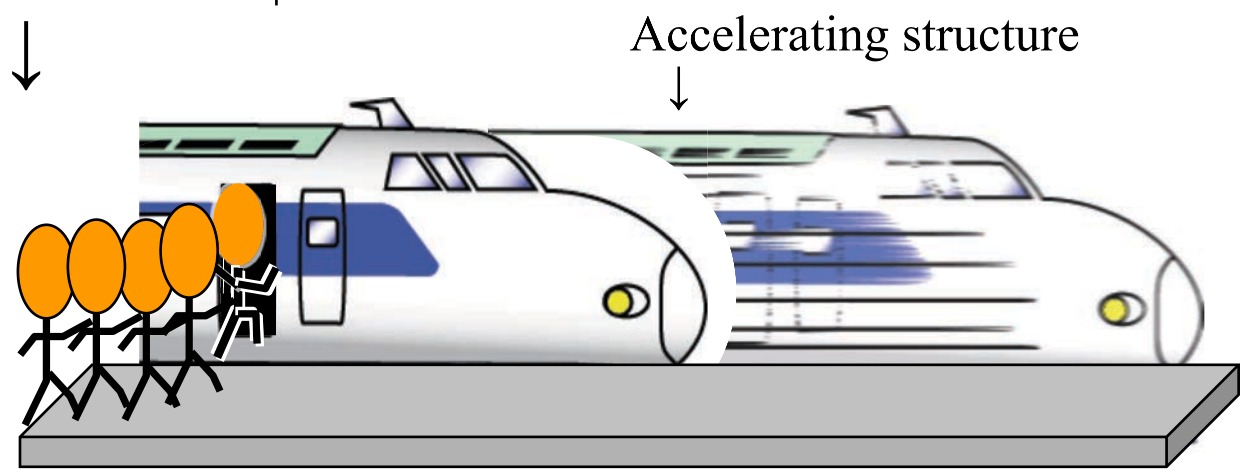

Efficient when <u>gradually</u> accelerated

Lesson #1: gradual acceleration → Relevant for ions

Adiabatic (Shinkansen) acceleration (2)

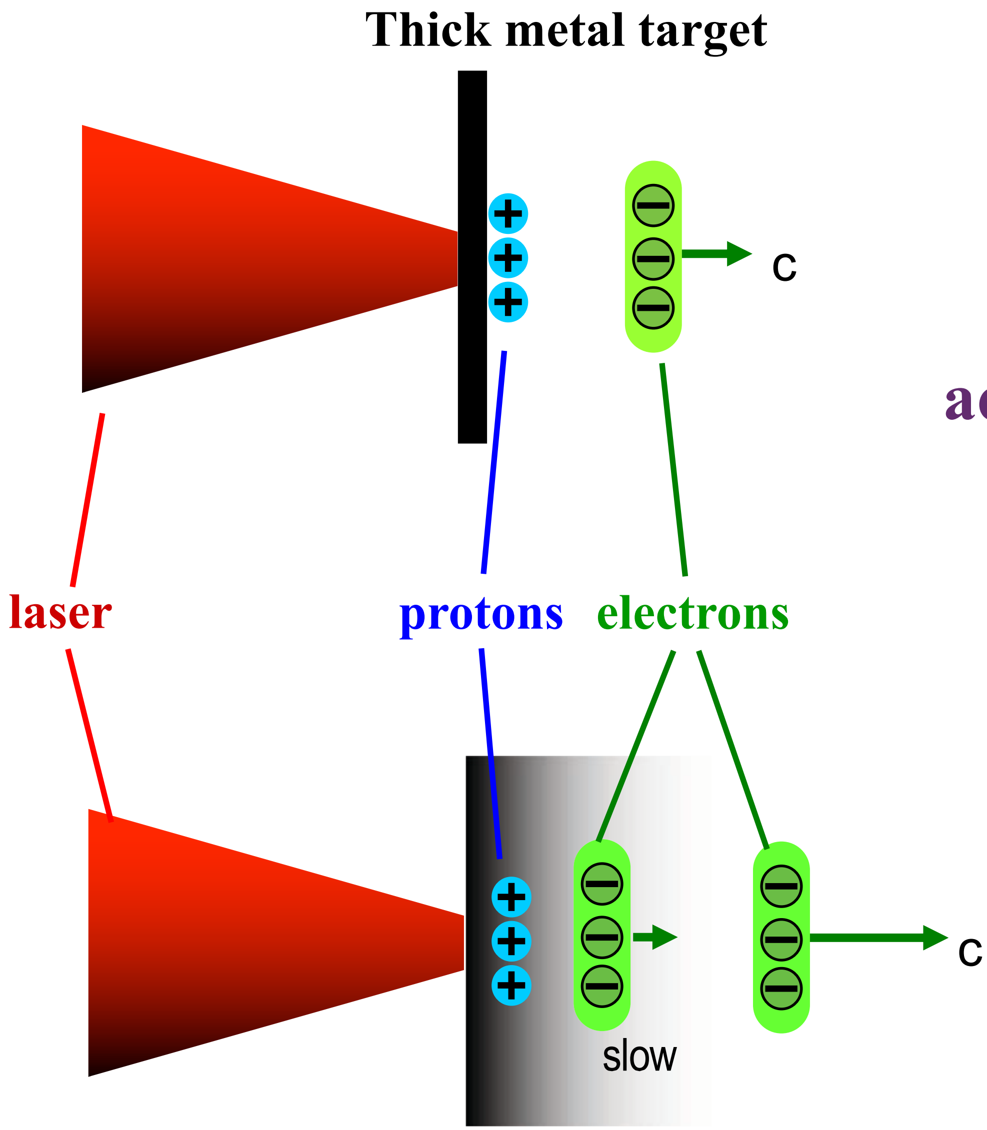

Graded, thin (nm), or clustered target and/or circular polarization

Most experimental configurations of proton acceleration(2000-2009)

Innovation ("Adiabatic Acceleration") (CAIL, 2009-)

= Method to make the electrons within ion trapping width

Target thickness scales with a_0

Coherent Acceleration of Ions by Laser (CAIL)

Deuteron energy vs. thickness of foil

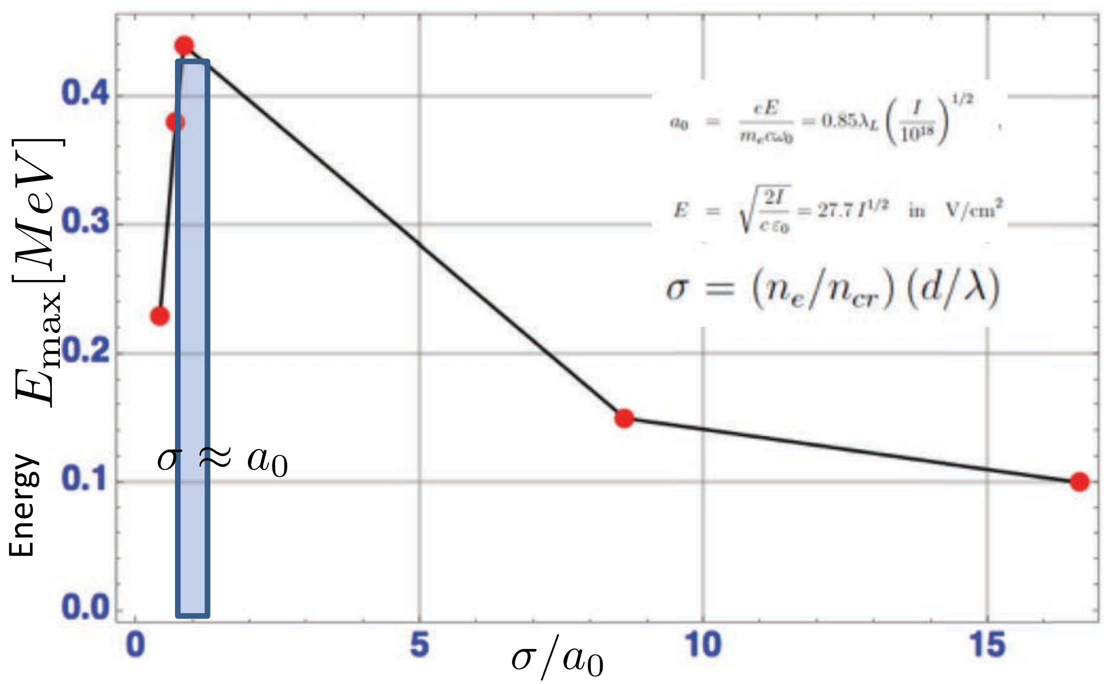

target thickness [normalized to laser intensity]

Our simulation

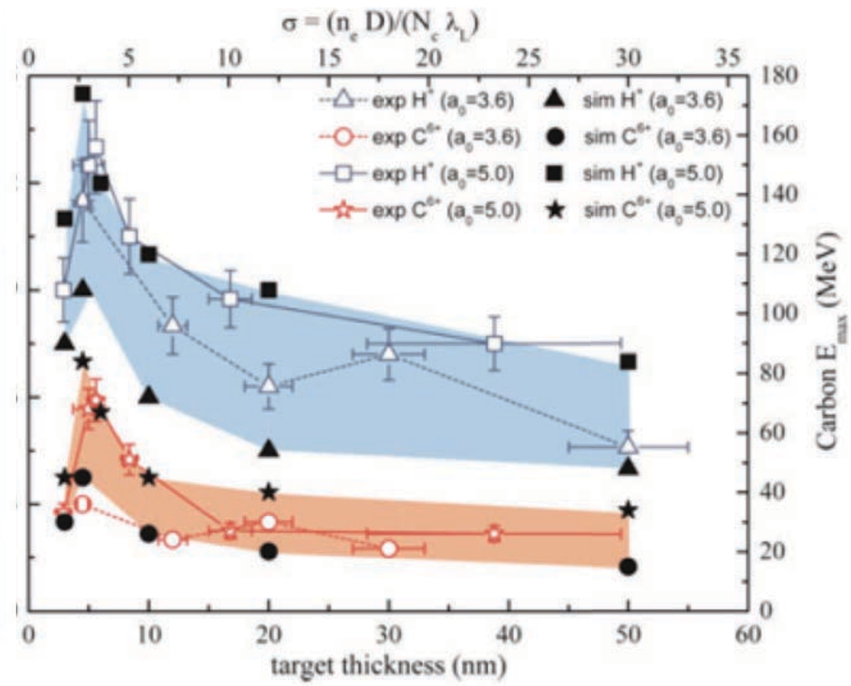

Experiment: Steinke (2010)

Optimum parameters (sweet-spot) for ion acceleration at $\sigma \approx a_0$

Necas (2018)

Laser accelerator (CAIL) : Efficient coupling to ions

The shorter the laser pulse, the higher deuteron acceleration (totally different from TNSA)
Very little energy needed per laser pulse (mJ).

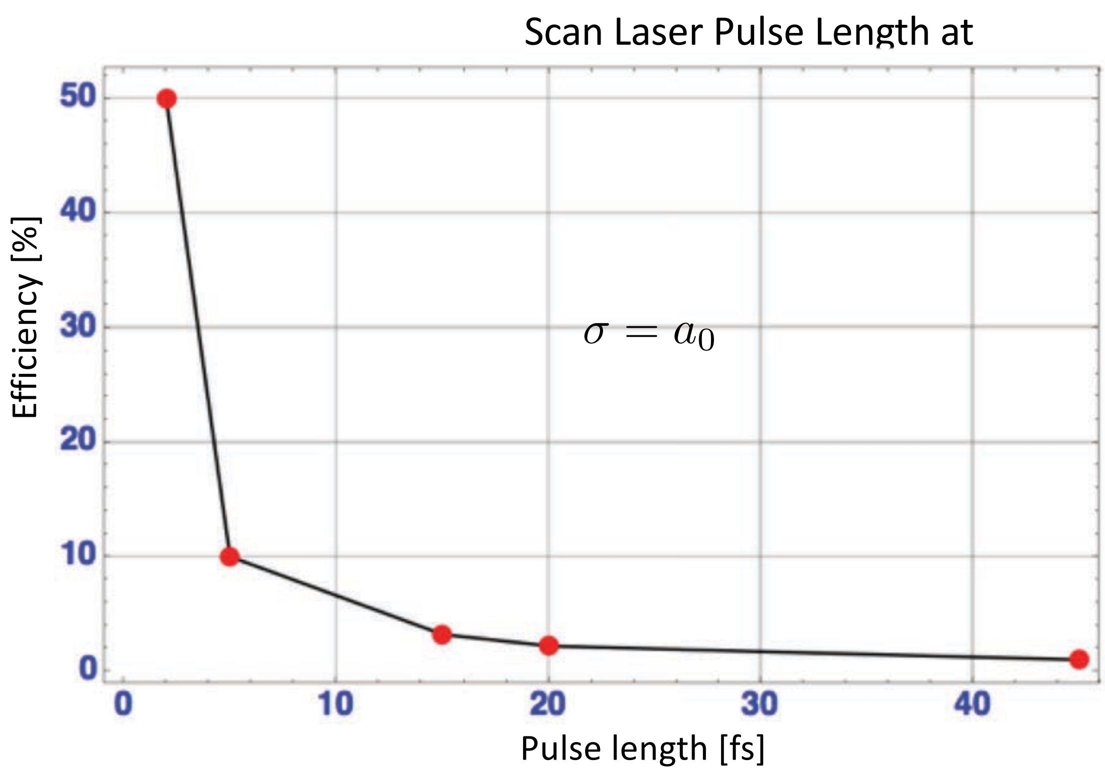

$$a_0 = \frac{eE}{m_e c \omega_0} = 0.85\lambda_L \left(\frac{I}{10^{18}}\right)^{1/2},$$

$$E = \sqrt{\frac{2I}{c\varepsilon_0}} = 27.7\, I^{1/2} \quad \text{in} \quad \mathrm{V/cm^2}$$

$$\sigma = (n_e/n_{cr})\,(d/\lambda)$$

$$\omega_L = \frac{2\pi c}{\lambda}$$

$$n_{cr} = \epsilon_0 m_e \omega_L^2 / e^2$$

$$\sigma = a_0$$

Short pulse ➡ **high** efficiency coupling

➡ societal applications (see next)

自己責任を果たす新しい哲学とサイエンス

New Philosophy and Science to Fulfill Self-responsibility

20th Century:
Science of Discovery

↓

21st Century:
Toilet Science:
Responsive to
societal issues
self-inflicted

Tajima
(Jan. 18,2005)

Toilet Science with CAN laser :
Coherent Acceleration of Ions by Laser (CAIL)

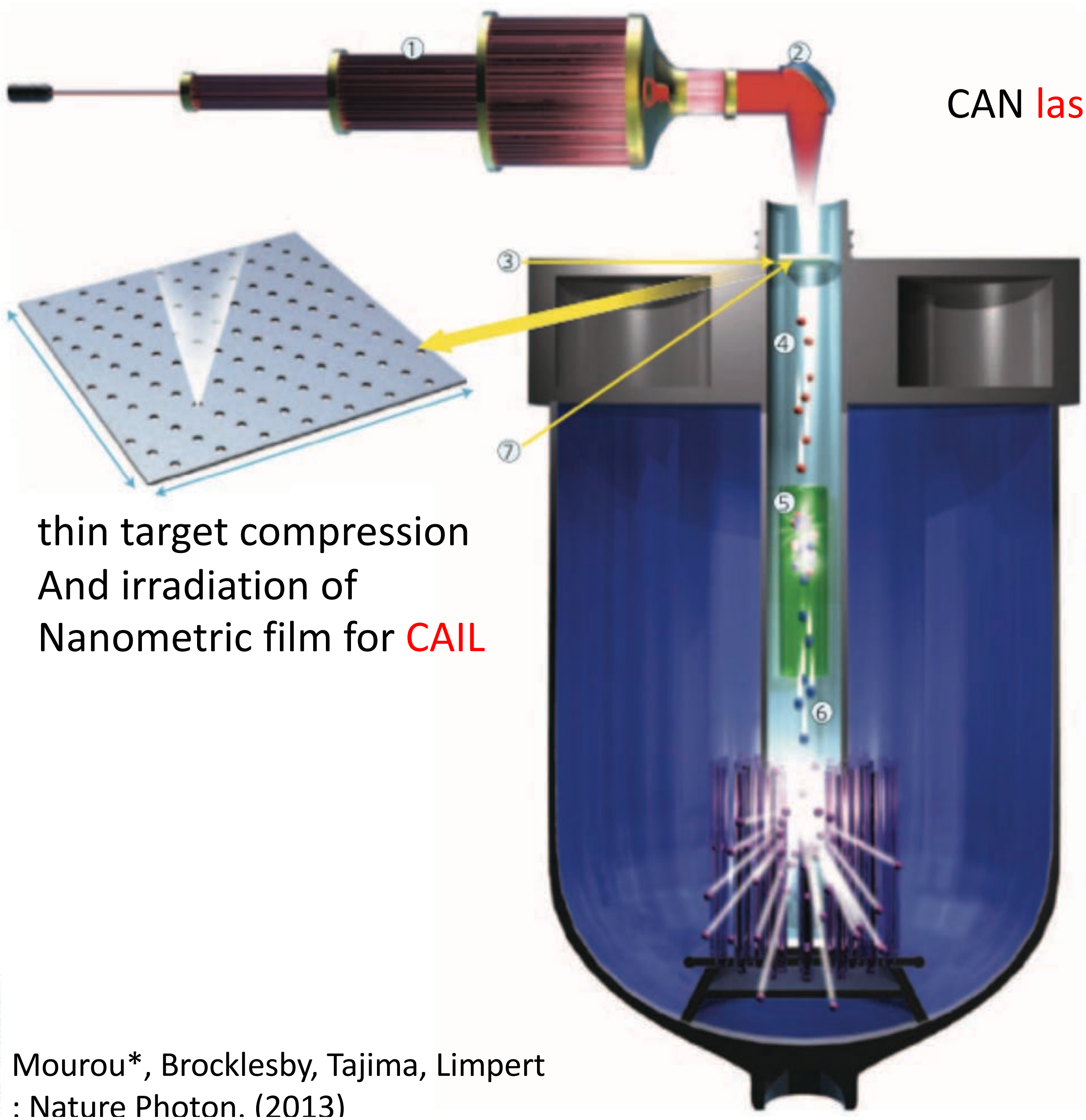

CAN laser

thin target compression
And irradiation of
Nanometric film for CAIL

Transmutator of nuclear waste
by neutrons
(Tajima, Necas, Mourou*, Gales,
Leroy, 2018)

generated with deuteron
acceleration by CAIL
(Tajima, Yan, Habs, 2010)

Mourou*, Brocklesby, Tajima, Limpert
: Nature Photon. (2013)

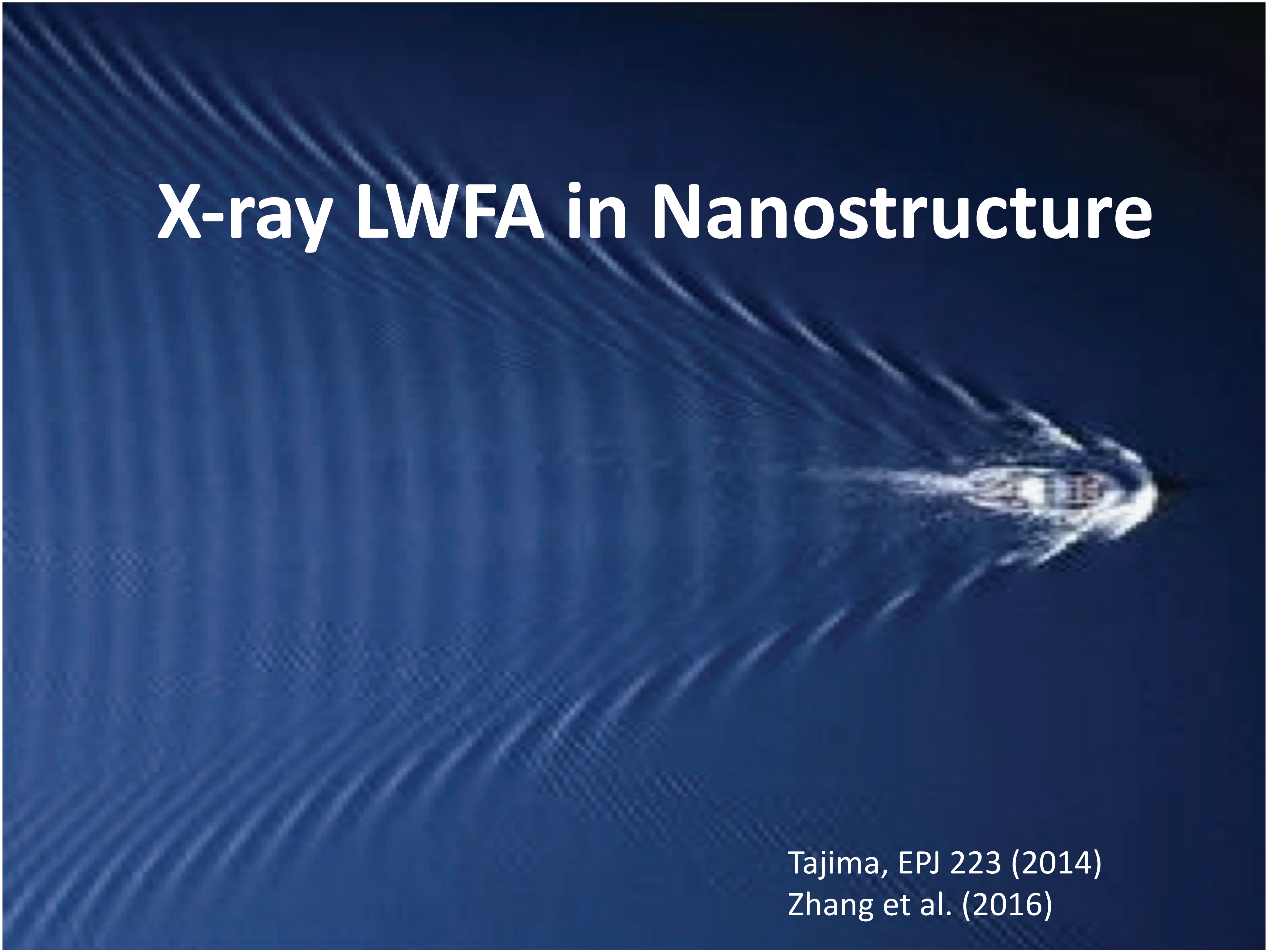
X-ray LWFA in Nanostructure
Tajima, EPJ 223 (2014)
Zhang et al. (2016)

Relativistic Compression

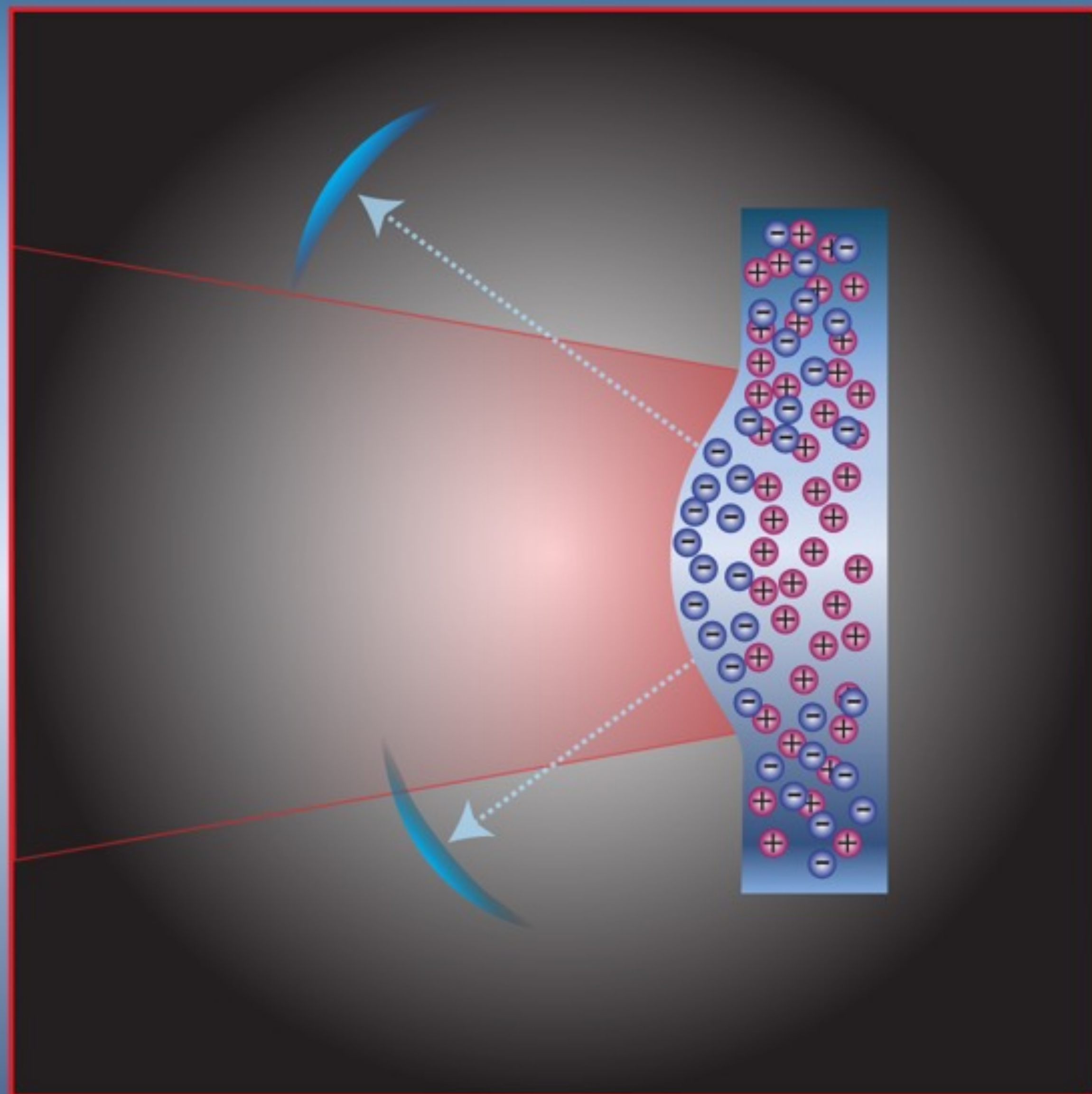

Thin Film Compression (TFC) into a Single-Cycled Laser Pulse

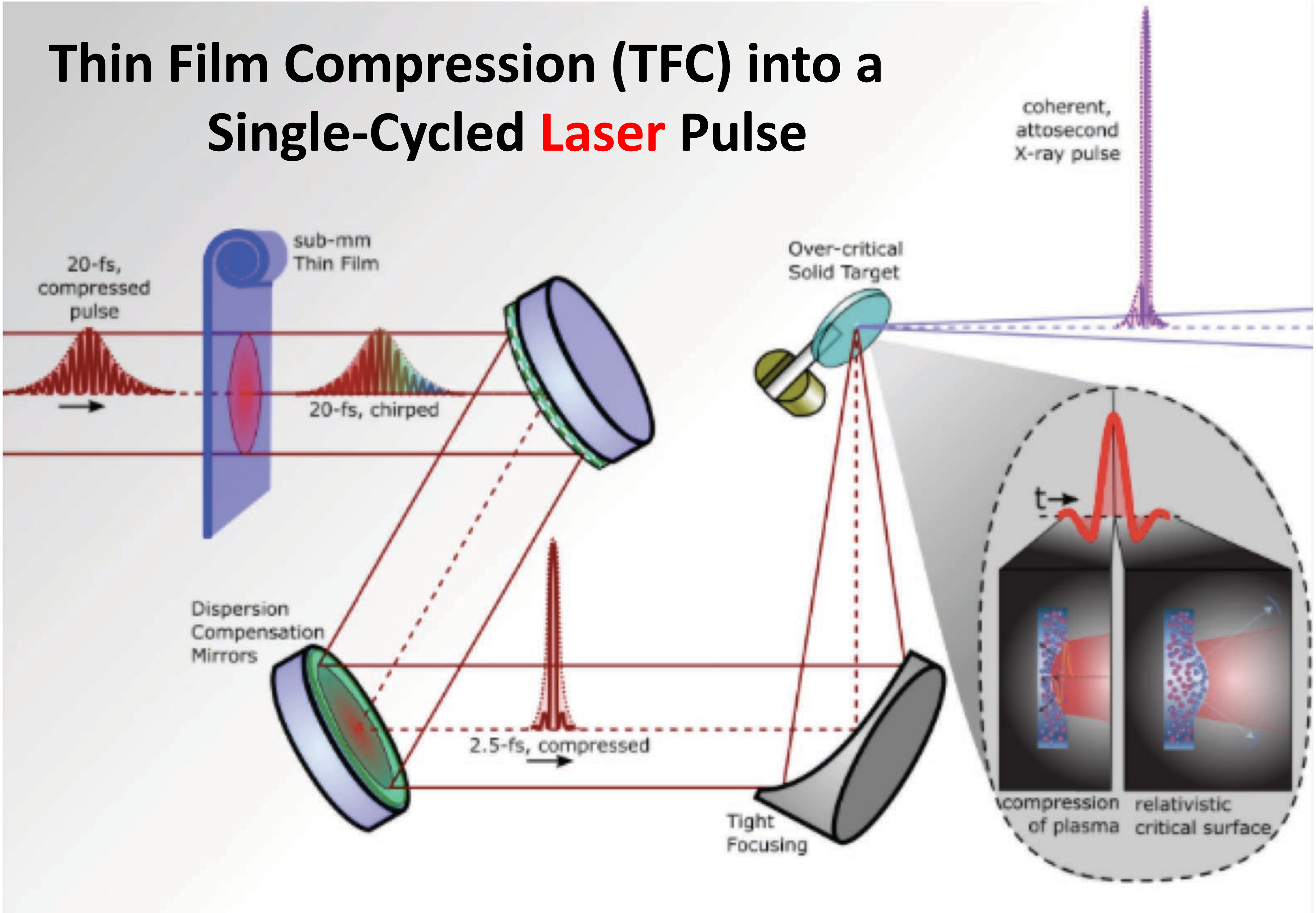

Mourou* , Brocklesby, Tajima, Limpert (2014)

Porous Nanomaterial:

rastering possible

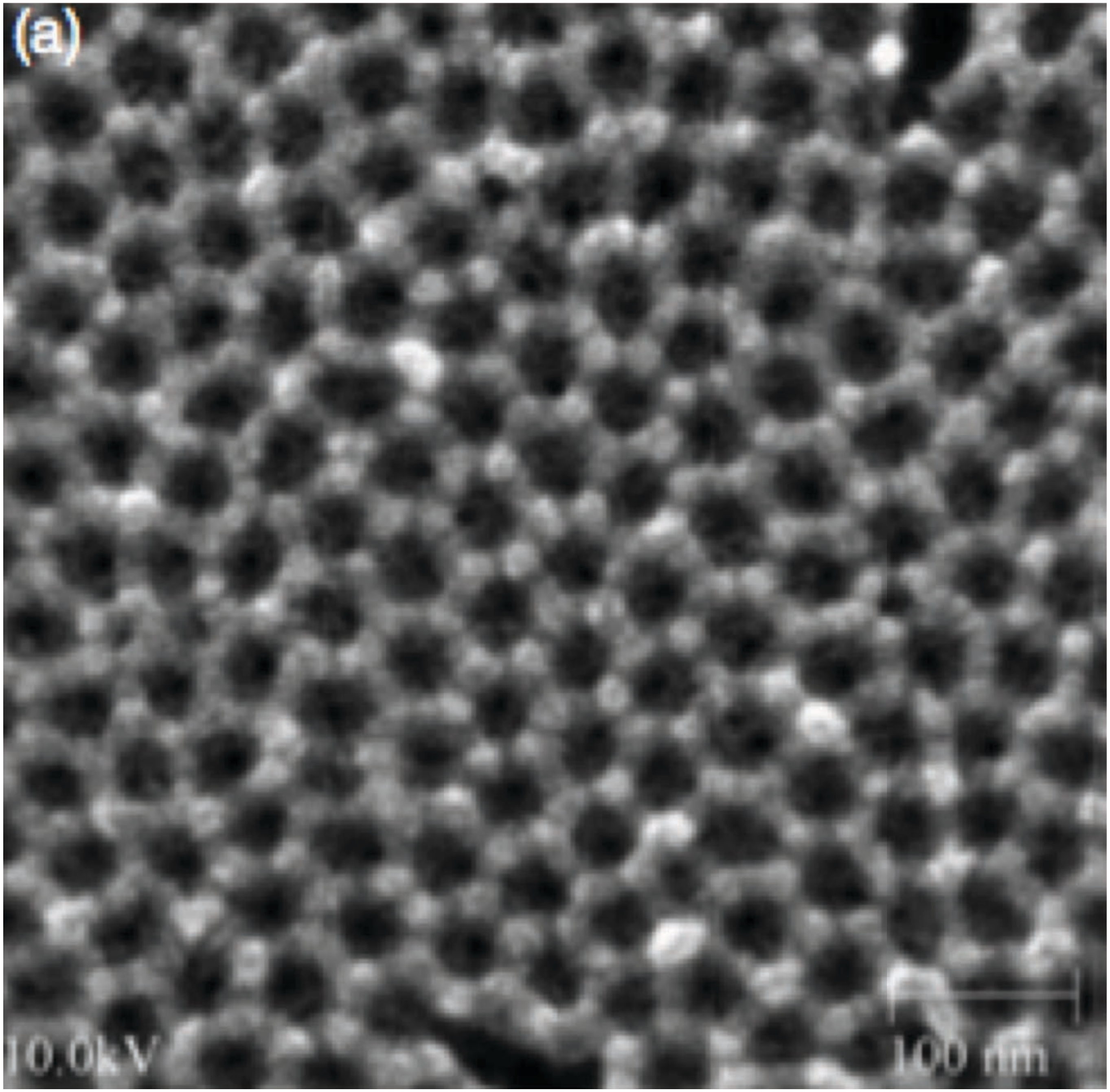

Nano holes:

reduce the stopping power

keep strong wakefields

➔ Marriage of *nanotech* and *high field science*

Spatia (nm), time(as-zs), density 10^{24} /cc), photon (keV) scales:

Transverse and longitudinal **structure of nanotubes**: act as e.g., accelerator structure (the structure intact in time of ionization, material breakdown times fs > x-ray pulse time zs-as)

Porous alimina on Si substrate Nanotech. **15**, 833 (2004);
P. Taborek (UCI): porous alumina (2007)

Fermilab/UCI efforts on nanostructure wakefield acceleration

16th Advanced Accelerator Concept Workshop (AAC2014)

TeV/m Nano-Accelerator

Current Status of CNT-Channeling Acceleration Experiment

Y. M. Shin[1,2], A. H. Lumpkin[2], J. C. Thangaraj[2], R. M. Thurman-Keup[2], P. Piot[1,2], and V. Shiltsev[2]

Thanks to X. Zhu, D. Broemmelsiek, D. Crawford, D. Mihalcea, D. Still, K. Carlson, J. Santucci, J. Ruan, and E. Harms

[1]Northern Illinois Center for Accelerator and Detector Development (NICADD), Department of Physics, Northern Illinois University

[2]Fermi National Accelerator Laboratory (FNAL)

X-ray wakefield acceleration in nanomaterials tubes

T. Tajima, EPJ (2014)

X-ray laser with short length and small spot:

NB: electrons in outers-shell bound states, too, interact with X-rays

Simulation: X.M. Zhang, et al.PR AB (2016)

Laser pulse with small spot can be well controlled and guided with a tube. Such structure available e.g. with **carbon nanotube,** or **alumina nanotubes** (typical simulation parameters)

$$\lambda = 1nm, a_0 = 4, \sigma_L = 5nm, \tau_L = 3nm / c$$

$$n_{tube} = 5 \times 10^{24} / cm^3, \sigma_{tube} = 2.5nm$$

Wakefield comparison between the cases of a tube and a uniform density

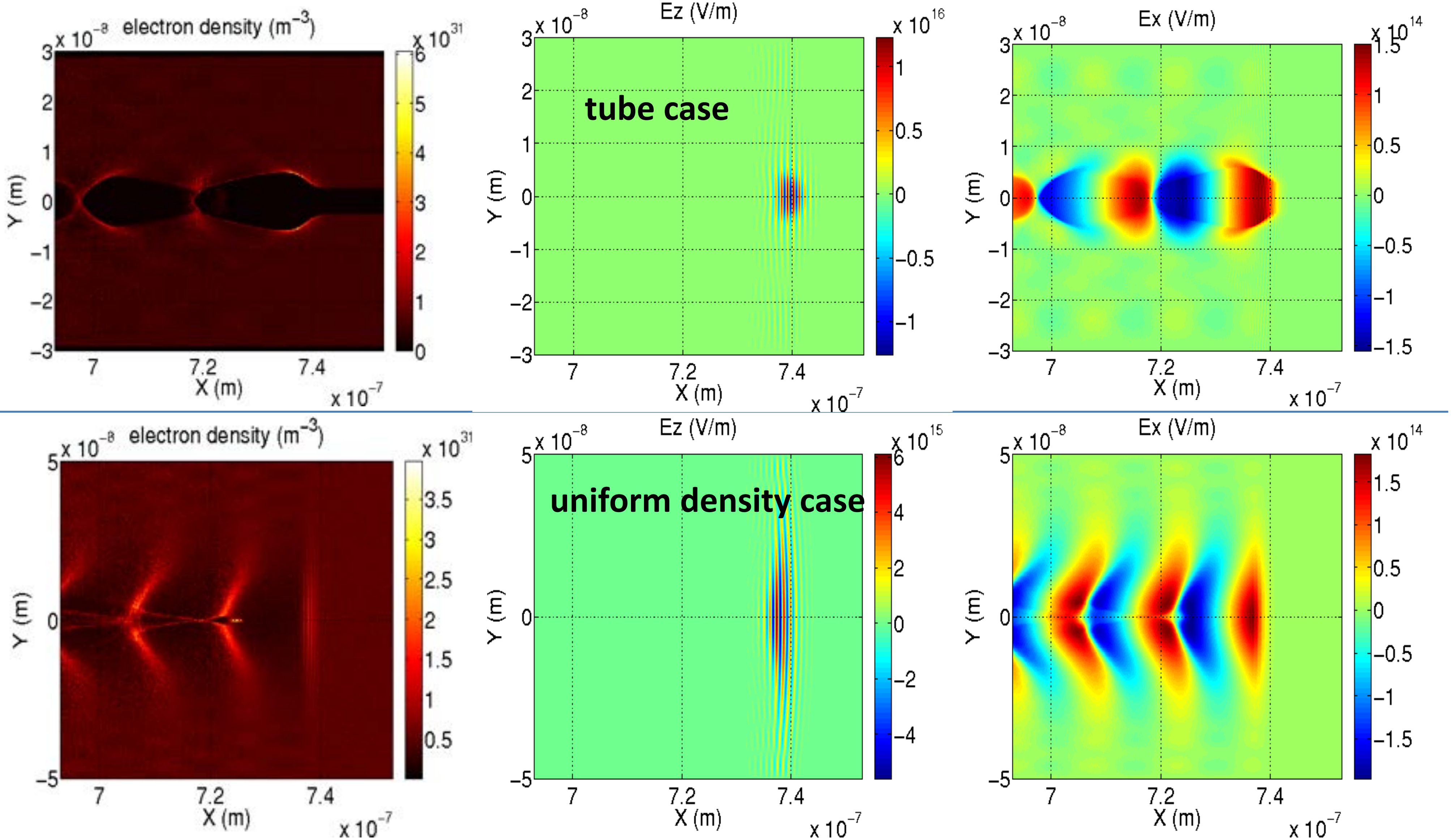

X. M. Zhang, Tajima,…Mourou*,… (2016)

With and without optical phonon branch

Model of optical phonon branch: *T. Tajima and S. Ushioda, PR B (1978)*

→ nanoplasmonics in X-ray regime

Without lattice force (i.e. plasma)

(when ω_{TO} is much smaller than ω_{pe}, there is no noticeable difference from the below where $\omega_{TO} = 0$)

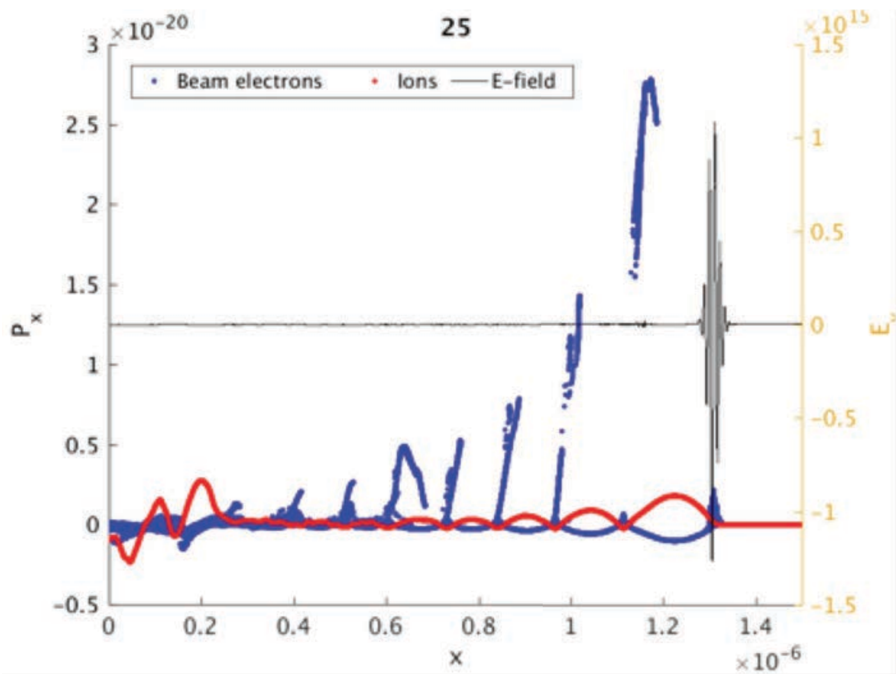

With lattice force (optical phonon branch present)

$$\epsilon = 1 - \frac{\omega_{pe}^2}{\omega^2} - \frac{\Omega_p^2}{\omega^2 - \omega_{TO}^2}$$

$$\frac{\omega_{TO}}{\omega_{pe}} \simeq 0.75 \qquad \frac{\Omega_p}{\omega_{pe}} \simeq \frac{1}{43}$$

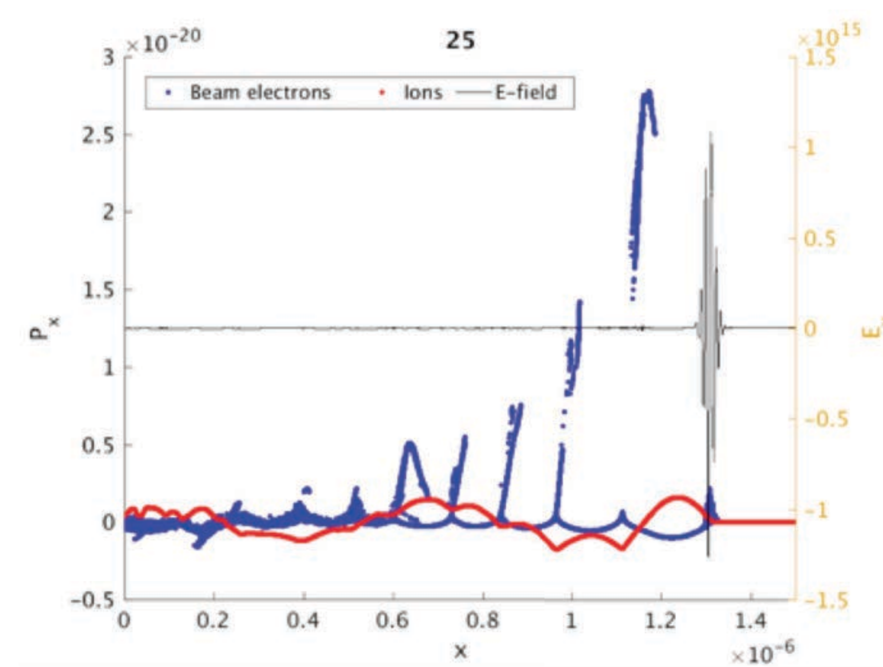

S. Hakimi, et al. (2017)

Wakefield on a chip

toward TeV over cm (beam-driven)

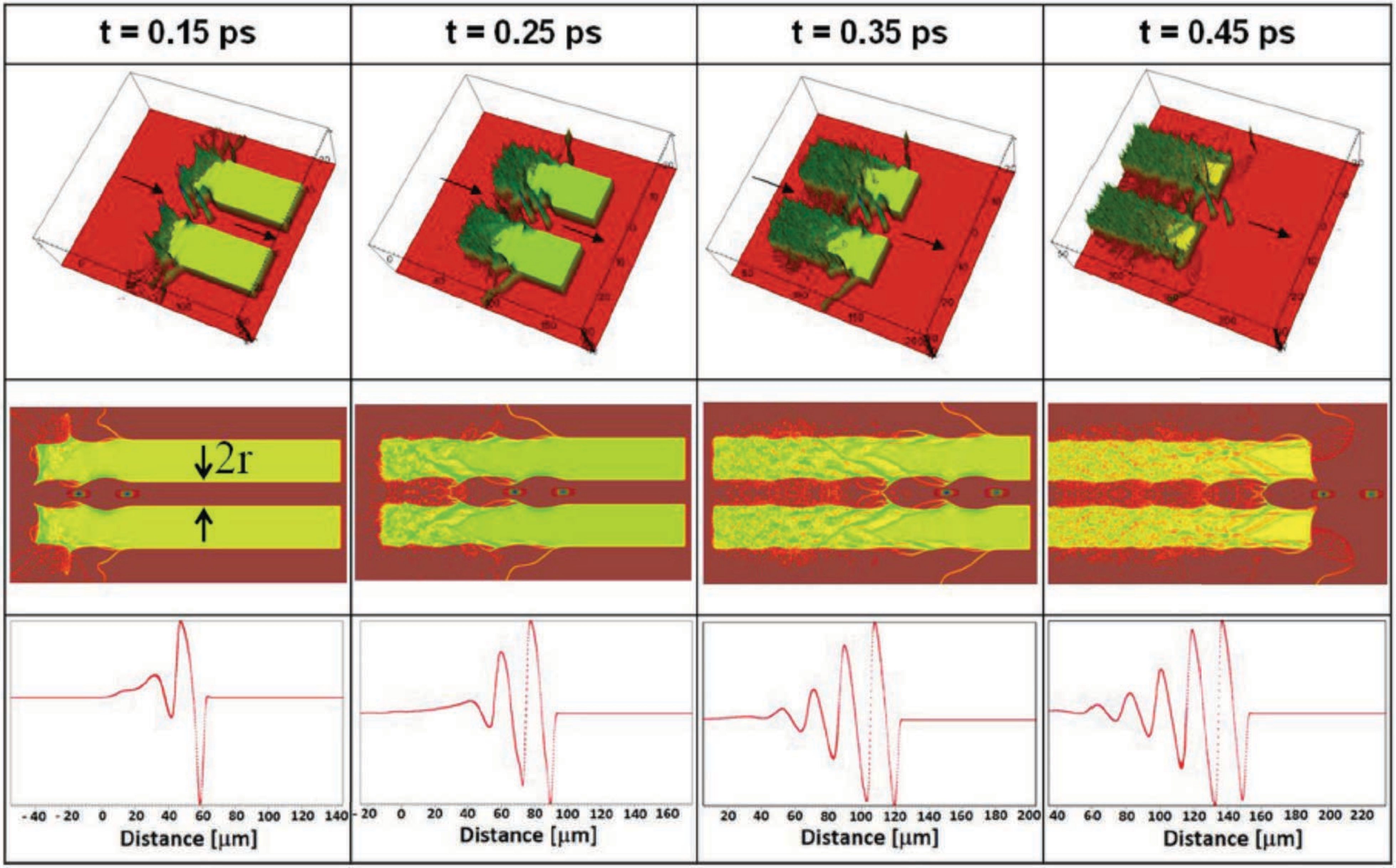

Y. Shin (2014)